EFFECTS OF THE NORTH PACIFIC OSCILLATION AND ENSO ON SEASONALLY AVERAGED TEMPERATURES IN CALIFLORNIA

David W. Pierce

CCCC/CAP Report 3.0
February 2004

California Climate Change Center
Funded by the California Energy Commission

California Applications Program
Funded by NOAA Office of Global Programs

Information for California's decision makers

.

The CCC/CAP Report Series provides timely access to scientific research concerning Califronia's climate and environment from:

California Climate Change Center (CCCC)

The California Climate Change Center aims to evaluate, expand, and enhance projections of climate change for decision makers in California and the surrounding region. Established 2003; sponsored by the California Energy Commission.

California Applications Program (CAP)

http://meteora.ucsd.edu/cap

The California Applications Program (CAP) aims to develop and provide better climate information and forecast for decision makers in California and the surrounding region. By working directly with users, CAP is working to evaluate climate information needs and utility from the user perspective. Established 1998; sponsored by NOAA's Office of Global Programs.

Effects of the North Pacific Oscillation and ENSO on Seasonally Averaged Temperatues in California

David W. Pierce

Climate Research Division, Scripps Institution of Oceanography
La Jolla, California

2 Febuary 2004

ABSTRACT

The North Pacific Oscillation (NPO) and the El Nino-Southern Oscillation (ENSO) have effects on California that are of interest to energy producers and consumers. In particular, changes in the NPO are associated with statewide shifts in simulteneous wintertime temperatures, and, to a lesser extent, temperatures in the following summer. Observations over the period 1960 to 2001 indicate that the seasonally averaged temperature anomaly associated with the NPO is about 0.7 C in winter and 0.2 C in summer. The response is not linear; the warmth associated with positive NPO events is stronger than the cooling associated with negative NPO events. The seasonal temperature changes are accomplished by a simple shift in the distribution of daily average temperatures over much of California. Howver, over the Sierra Nevadas, the shape of the daily temperature distribution changes as well, with the positive phase of the NPO associated with a smaller standard deviation in daily average temperature. This effect is probably too small to be of practical importance for energy producers, however. The seasonally averaged difference in temperature due to the NPO makes about a 150 heating degree day difference over the winter. The change in seasonally averaged temperatures due to ENSO is a considerably weaker effect than that due to the NPO; effects on energy producers due to ENSO are therefore more likely to arise from changes in precipitation in the Pacific Northwest.

1. Introduction

Large-scale climate fluctuations such as the North Pacific Oscillation (NPO) and the El Nino-Southern Oscillation (ENSO) have systematic effects on California's temperature. Some of these effects are of interest to the energy industry. For example, colder winters result in greater demand for natural gas for space heating, while hotter summers result in greater peak electricity loads.

The purpose of this note is to quantify these effects, in both observations and in global climate models. Of particular interest will be the seasonality of the climate signal - warm summers present a very different energy stress than cold winters - as well as the manner in which the climate variability is accomplished (e.g., colder average winters being accomplished by the increased likelihood of a few very cold days versus many slightly cooler days). Both observations and models are evaluated so the fidelity of modeling studies of California's climate can be evaluated. Such modeling studies might be of global change due to anthropogenic effects over the coming decades, or of dynamical model predictions of California's climate on the seasonal timescale.

This note is organized as follows. In section 2 the NPO and ENSO are briefly described. The data sources are outlined in section 3. Section 4 describes the influence of the NPO on California, while section 5 examines the effect of ENSO. A summary is given in section 6, including conclusions that can be drawn about the ability of models to capture these climate signals over California.

2. Climate Indices

a. North Pacific Oscillation (NPO)

1) OBSERVATIONS

The NPO (Walker 1923,Walker and Bliss 1932) is a large scale fluctuation of atmospheric pressure and sea surface temperatures in the North Pacific. The observed wintertime sea surface temperature (SST) and sea level pressure (SLP)

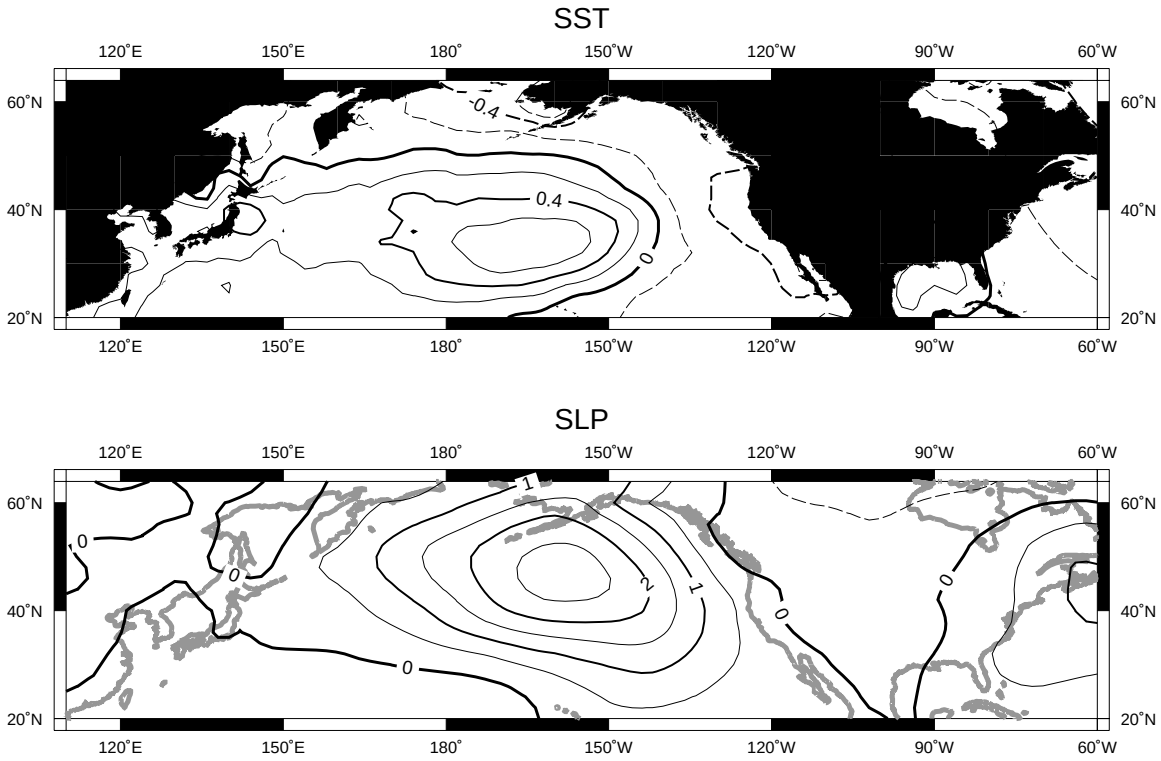

Figure 1: Observed winter (Dec-Jan-Feb) sea surface temperature anomaly (top, degrees C) and sea level pressure anomaly (bottom, millibars) associated with the North Pacific Oscillation, over the period 1949-2000.

anomalies associated with the NPO are illustrated in Figure 1. (Anomalies are departures from conditions normal for that time of year.) The NPO is also related to winter temperatures over North America (e.g., Latif and Barnett 1994; Trenberth and Hurrell 1994). The physical mechanism of the relationship is that high values of the NPO index are associated with southerly air flow along the west coast of North America, which tends to advect warmer southern air into the region (Trenberth and Hurrell 1994). Low values are associated with northerly flow, with the corresponding advection of colder, subpolar air into the region. Figure 1 illustrates the negative phase of the NPO. To a reasonable approximation, the positive phase is the opposite of the negative phase.

Various indices are used to describe the NPO, for example, an index of area-

weighted mean sea level pressure averaged over 30 N to 65 N, 160 E to 140 W (Trenberth and Hurrell 1994). The ”Pacific Decadal Oscillation” or PDO (Mantua et al. 1997) uses an index based on the leading empirical orthogonal function (EOF) of sea surface temperature (SST) anomalies in the Pacific, north of 20 N. In this work we will use the latter definition, taken over winter (December-January-February, or DJF), when the NPO is strongest. Values for the index can be obtained from http://jisao.washington.edu/pdo/PDO.latest.

The global SST dataset used here is the daSilva version of the COADS data set (da Silva et al. 1995), supplemented by National Centers for Environmental Prediction (NCEP) temperatures after 1993.

The sea level pressure data set is from the NCAR-NCEP reanalysis program, and covers the period 1949 to 2000.

Generally speaking, the NPO has a ”red” spectrum (Pierce 2001), with more energy in multiyear to decadal timescales than in annual timescales. This raises the possibility that persistence might yield usable forecast information for changes related to the NPO, despite the fact that the NPO itself has not been shown to be predictable. This long-timescale variability is reflected in the fact that the NPO tends to go through long periods when it is either predominantly positive or predominantly negative. For example, over the period 1947 to 1976 (years are indicated by the year of the January in the Dec-Jan-Feb average), there were 19 negative years and 11 positive years; during the period 1977 to 1998, there were 4 negative years and 18 positive years, and during the period 1999 to 2002 there were 4 negative years and 0 positive years.

2) Model Results

The model evaluated here is the Parallel Climate Model (PCM; Washington et al. 2000). This is a global coupled ocean-atmosphere general circulation model (O-A GCM) run at an atmospheric resolution of T42 (approximately 2.8^o in latitude and longitude), and an oceanic resolution of 384 gridpoints by 288 gridpoints (approximately $2/3^o$ resolution on average). The model includes a land surface

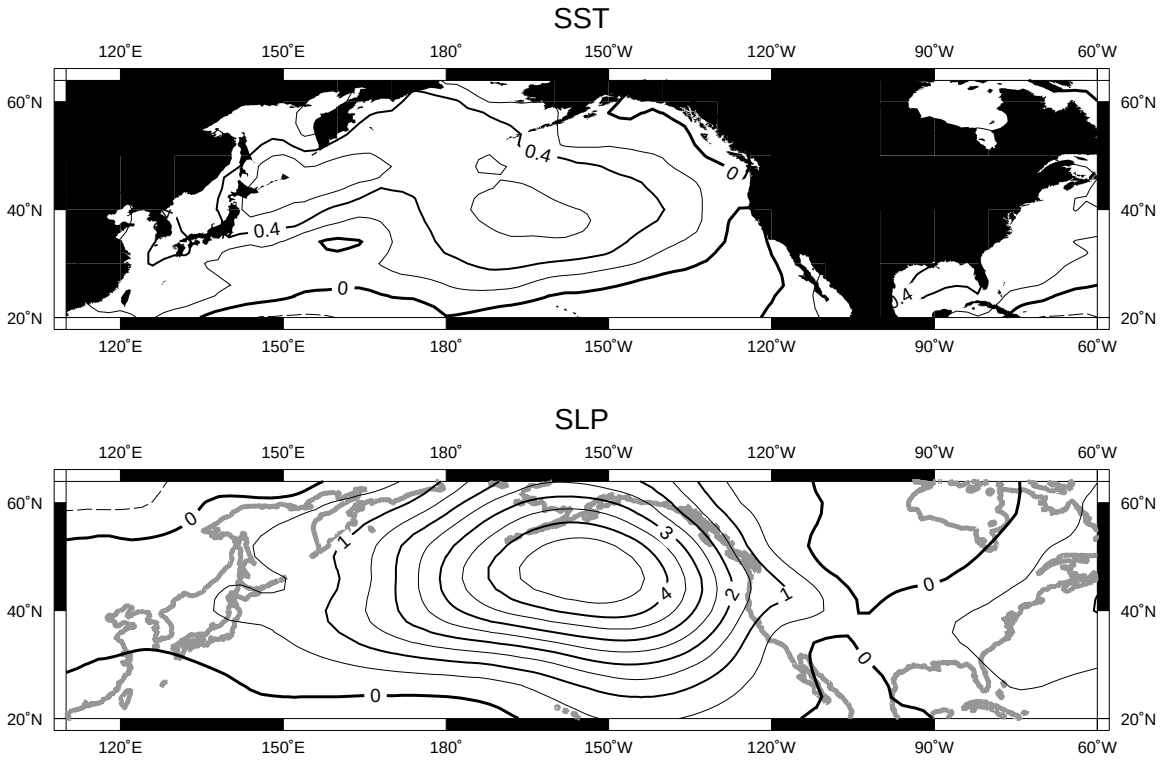

Figure 2: Modeled winter (Dec-Jan-Feb) sea surface temperature anomaly (top, degrees C) and sea level pressure anomaly (bottom, millibars) associated with the North Pacific Oscillation.

model with parameterized vegetation, and a full dynamic-thermodynamic sea ice model. The results shown here are from the "B06.62" control run, which is 600 years long. No flux correction is used in the model. PCM was the model used in the Accelerated Climate Prediction Initiative (ACPI) demonstration project Barnett et al. (2004), which evaluated future changes in the hydrological cycle of the west due to anthropogenic forcing. It was the use of PCM in the ACPI project that motivates its use here (in the context of energy issues), as hydropower is an important source of power for the western U.S. electrical grid.

The model's version of the NPO is shown in Figure 2. The model captures the strength of the SST anomaly pattern accurately (about 0.6 ^{o}C), although the pattern of warm anomalies extends about 20 degrees too far to the east. The SLP anomaly is a stronger in the model than observed (5 mb vs. 3 mb), which might

have the tendency to exaggerate the wind anomalies associated with the NPO. The location and pattern of the SLP anomaly closely matches that observed.

b. El Nino-Southern Oscillation (ENSO)

The El Nino-Southern Oscillation (ENSO) is a large-scale, coupled ocean-atmosphere climate fluctuation that originates in the equatorial Pacific ocean. It is so named because it was found that the oceanic cycle of El Ninos and La Ninas, and the atmospheric cycle of the Southern Oscillation, are different parts of the same coupled ocean-atmosphere phenomenon. An El Nino is associated with warmer than usual water in a strip along the central to eastern tropical Pacific and enhanced large-scale convection (storm activity) in the same region. A La Nina, by contrast, is associated with colder than normal water in the central tropical Pacific. Although ENSO itself is confined to the tropical Pacific, atmospheric waves can carry ENSO's effects into the extratropics, leading to responses there that are typically called "El Nino" or "La Nina." The remote response is typically strongest in the winter hemisphere, i.e., between December and March over North America.

The index of ENSO used here is called the "Nino 3.4 index," and is the sea surface temperature anomaly averaged over the region 5 S to 5 N, 180 to 140 W. Figure 3 (top panel) shows the regression of the observed nino 3.4 index on global SST anomalies; the characteristic signature of El Nino, the tongue of warmer than usual water in the tropical Pacific, is easily seen. La Nina has a similar pattern, but with the opposite sign.

There is no fixed standard for when an El Nino or La Nina exists, partly because different parts of the world are sensitive to different locations of remote forcing in the tropics, and partly because different locations are sensitive to ENSO's effects at different times of the year. For North America, a useful and practical definition of an El Nino is when the Nino 3.4 SST index is greater than 0.5 C, and a La Nina is when the index is less than -0.5 C.

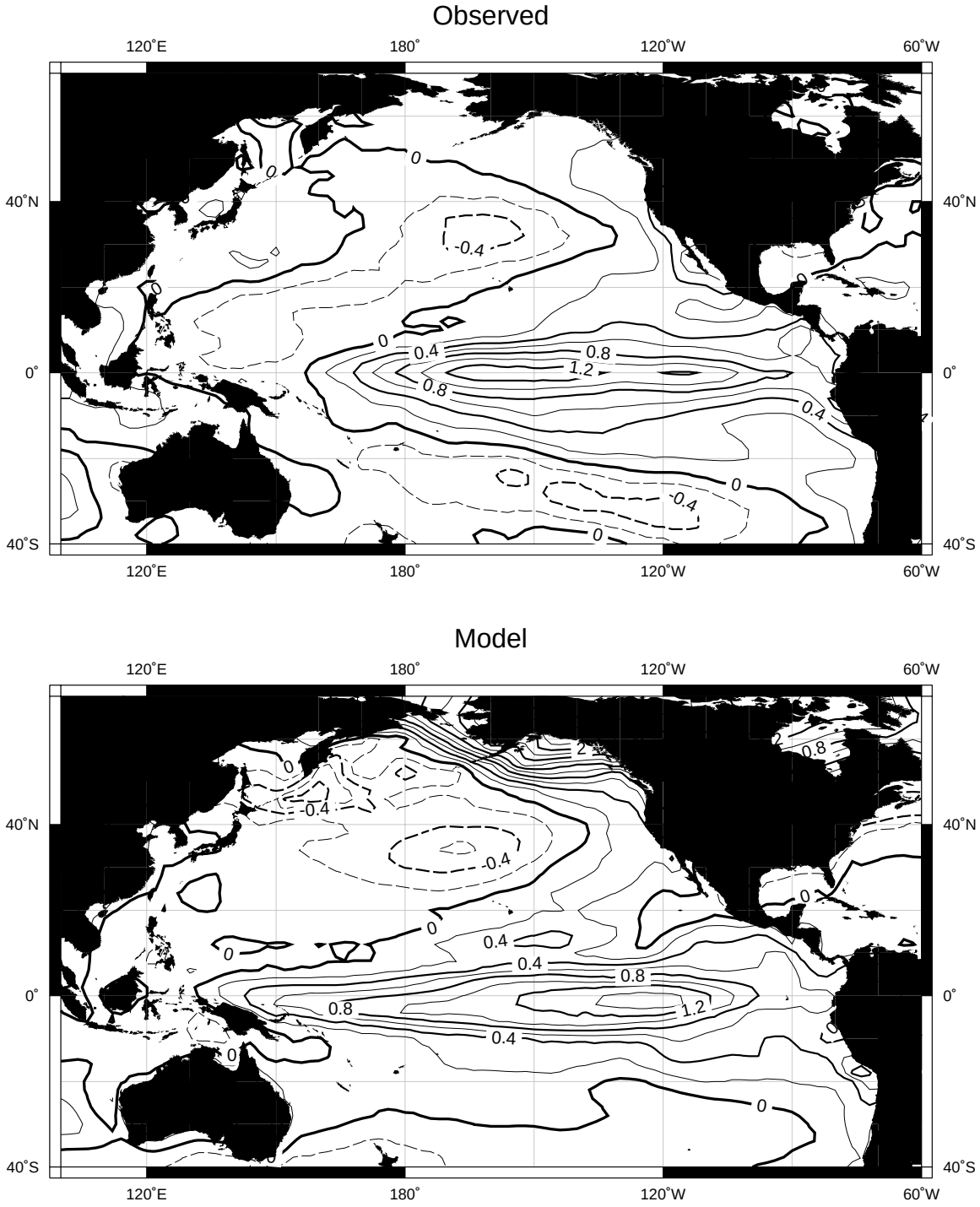

Figure 3: Regression pattern (^{o}C) between the DJF nino3.4 index and DJF SST anomalies over the Pacific ocean.

The model has an ENSO cycle that is similar to that observed, but extends too far to the west (Figure 3, bottom panel). This is a common failing in numerical O-G GCMs (Mechoso et al. 1995) for reasons that are not clear. Otherwise, the amplitude of the model's ENSO cycle is quite similar to that observed, both along the tropical strip and in the central North Pacific. The model has an exaggerated response in the Gulf of Alaska, however.

3. Data sources

The station data used here is primarily from the Groisman (pers. comm.) data set of station data throughout the United States. California stations were selected from the criterion that no more than 10% of the data values (minimum and maximum temperature) could be missing for the period of interest, 1960 to 2001. One hundred and thirty-four stations passed this criterion. The average temperature for the day was calculated as the average of the station's minimum and maximum temperatures.

For presentation of station data, a subset of the full set of California stations is shown. The stations used are based upon those used by those used by California Energy Commission (CEC) for their climate and weather modeling, and are intended to be representative of local climate conditions ("climate zones"). The 12 stations included are shown in Table 1. San Jose International Airport (COOP station ID 047824) is used by the CEC as a climate zone station, but does not appear in the Groisman data set. Data for this station were downloaded from http://nndc.noaa.gov/?http://ols.nndc.noaa.gov/plolstore/plsql/olstore.prodspecific?prodnum=C00122-MAN-S0001 (accessed 31 July 2003).

Heating and cooling degree days (HDD and CDD) are calculated from the station data using a baseline of 65F. In other words:

$$\mathrm{CDD} = \max(\frac{T_{min} + T_{max}}{2} - 65, 0) \quad (1)$$

$$\mathrm{HDD} = \max(65 - \frac{T_{min} + T_{max}}{2}, 0) \quad (2)$$

Station name	COOP-ID	Lat (N)	Lon (W)	HDD	CDD
Eureka WFO Woodley Is.	042910	40.8	124.15	4108	-
Ukiah	049122	39.13	123.2	-	881
Sacramento FAA airport	047630	38.52	121.5	2433	1255
Fresno Yosemite Int'l	043257	36.77	119.72	2249	2082
San Francisco WSO AP	047769	37.62	122.38	2583	164
Long Beach	045085	33.82	118.15	-	1201
Los Angeles WSO ARPT	045114	33.93	118.4	1207	-
San Diego WSO airport	047740	32.73	117.17	1124	767
Burbank-Glendale-Pasadena AP	041194	34.2	118.37	1388	1432
Blythe	040924	33.62	114.6	1034	4315
San Bernardino F S 226	047723	34.13	117.25	1445	1966
San Jose Int'l airport	047824	37.36	121.93	2054	835

Table 1: Stations used to represent California "climate zones."

where the daily minimum and maximum temperatures, Tmin and Tmax, are given in degrees Fahrenheit. As they are defined from the point of view of an energy generator, a "cooling degree day" is related to high air conditioner use, and so large CDD tend to occur in the summer. A "heating degree day" is related to high furnace or heater use, and large HDD tend to occur in winter.

Many of the station data showed strong trends over the period of record. Part of this is presumably due to urban heat island effects, which are not of interest here. Therefore, all the station data were detrended before use.

4. Influence of NPO on California temperatures

The influence the NPO has on California temperatures will first be shown by histograms at the stations representing the climate zones, stratified by phase of the NPO, and then as regressions across the entire state.

a. Histograms of HDD and CDD by phase of the NPO

The main effects of the NPO are felt during winter, however, for the purposes of the energy industry it is useful to examine summer as well. In this section winter will be taken as the average from October to March, while summer will be taken as the average over May to September. It should be kept in mind that the NPO index used here is based on winter conditions, so the analysis is simultaneous for the winter but incorporates a degree of persistence for the summer. In other words, the summer conditions are evaluated based upon the preceding winter's NPO.

Figure 4 shows HDD and CDD distributions for the positive and negative phases of the NPO. HDD and CDD values are anomalies from mean seasonal values, where winter (Oct-Mar) is used for HDD and summer (May-Sep) is used for CDD. Also shown is the average value of the anomaly obtained when the NPO is in the positive and negative phase. Table 1 shows the mean HDD and CDD values for the 12 climate zone stations, so that the size of the anomalies can be evaluated. Roughly speaking, the NPO makes a difference of about 5% to HDD (wintertime conditions), somewhat less than that in summer.

The possibility that the difference in HDD and CDD between the positive and negative phases of the NPO (NPO+ and NPO-) arises solely out of sampling fluctuations should be considered. This can be evaluated by using a Kolmogorov-Smirnov (K-S) test, which estimates the likelihood that the NPO+ and NPO- distributions are actually drawn from the same underlying distribution, and differ only due to chance, given the relatively short period of analysis (42 years). The results of the K-S tests are shown in Figure 4. Small numbers mean that it is unlikely that the observed differences arise by chance. For example, the top left panel of Figure 4 indicates that there is only a 1 in 10,000 (0.0001) chance that the observed difference in HDD distributions in Eureka would be found by chance. On the other hand, the top right panel (Eureka CDD) shows that there is almost a 50% chance of getting this result by chance. The data therefore support the conclusion that the NPO affects wintertime conditions in Eureka (HDD), but not

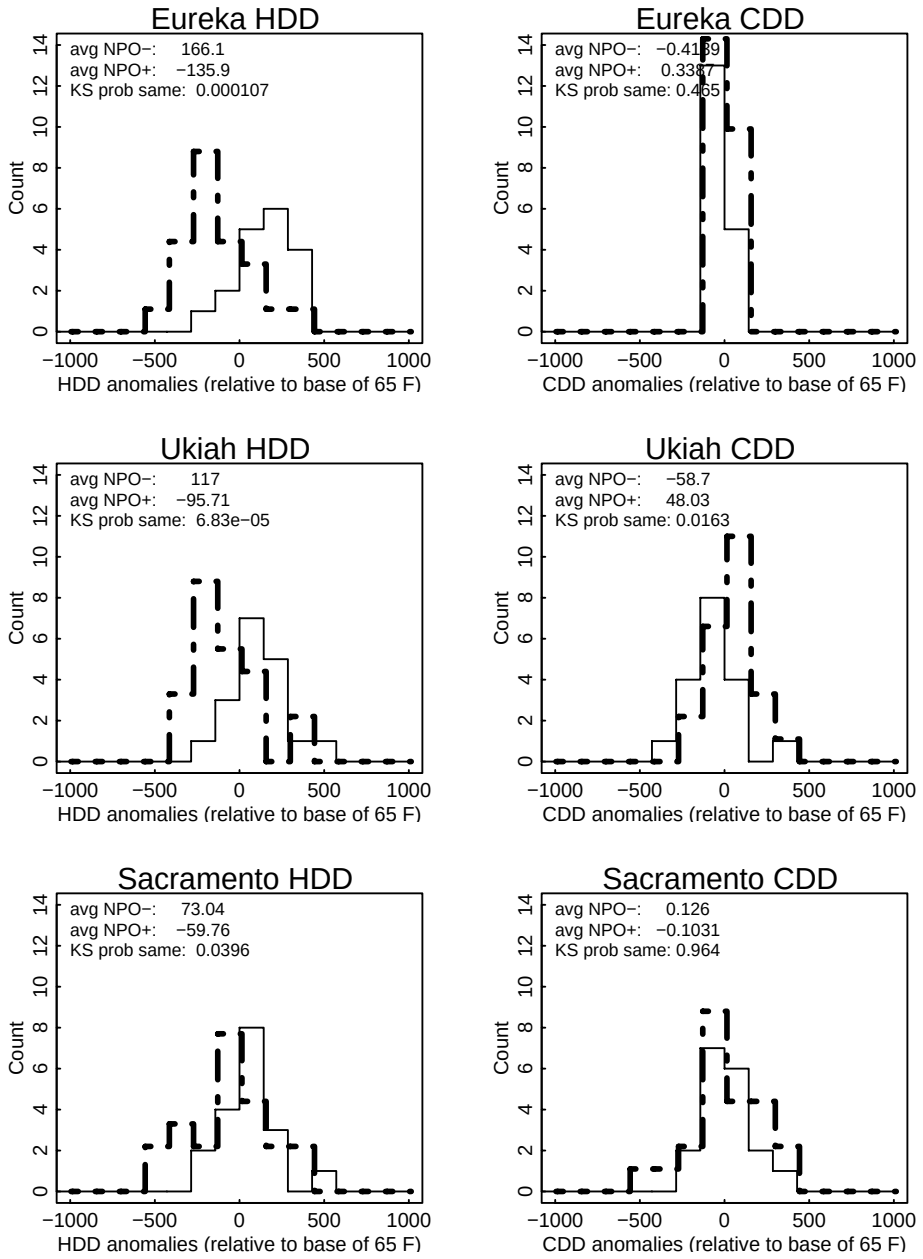

Figure 4a: HDD (left column) and CDD (right column) distributions for stations representative of California climate zones. The distribution for the positive phase of the NPO are shown by the heavy dashed line; for the negative phase of the NPO, by the thin solid line. Data has been detrended before analysis; departures from mean conditions are shown. HDD values are winter (Oct-March) average, CDD values are summer (May-Sep) averages.

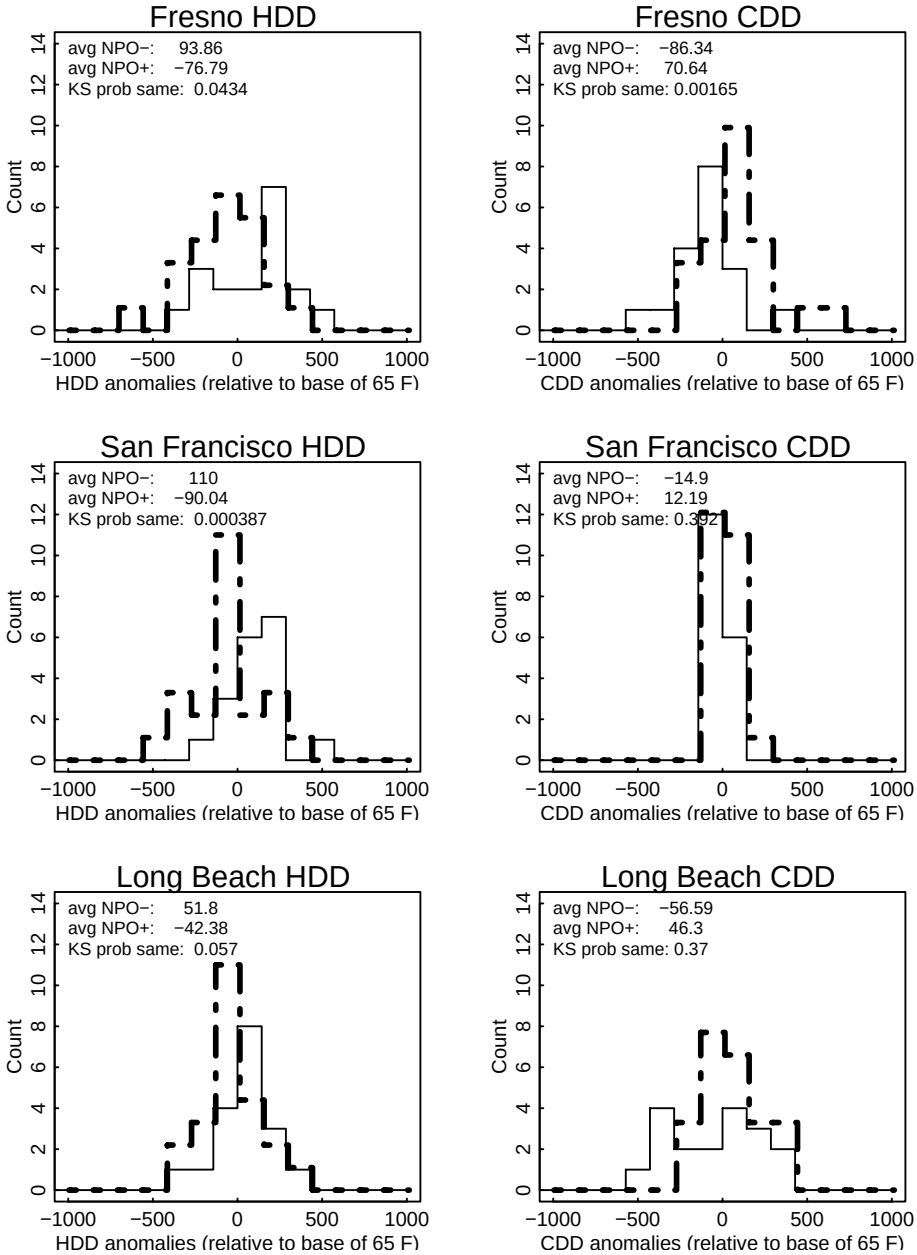

Figure 4b: continued.

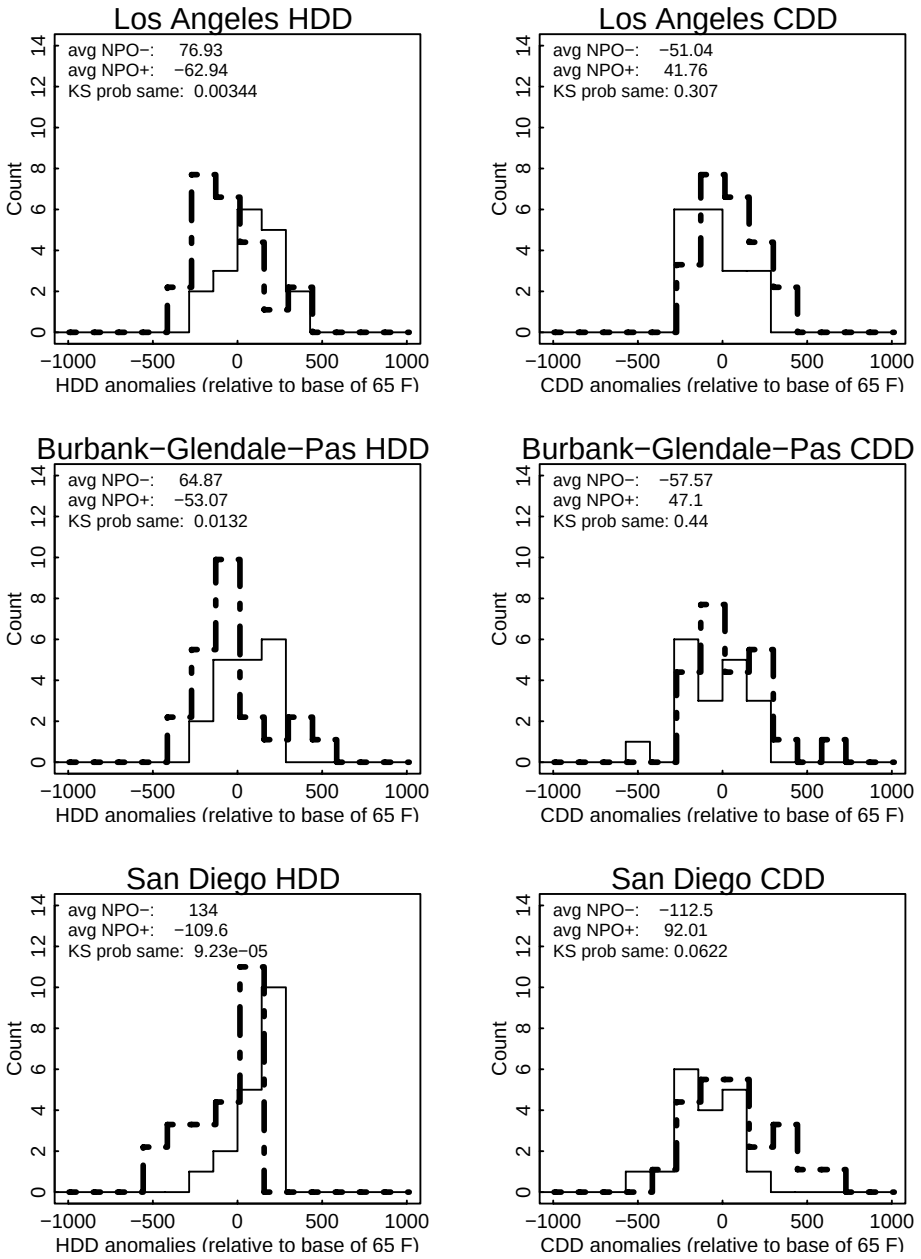

Figure 4c: continued.

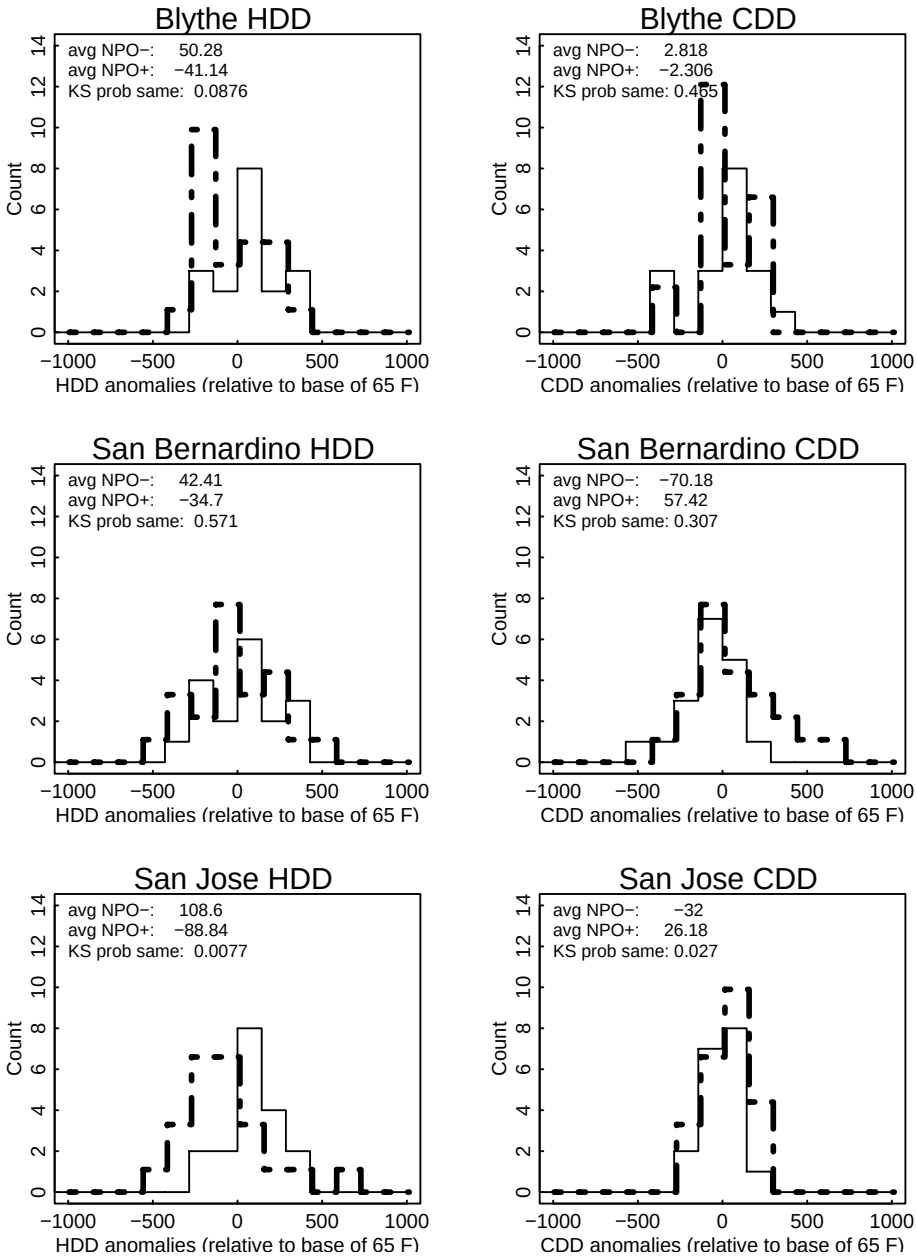

Figure 4d: continued.

summertime conditions (CDD).

Overall, nine of the twelve climate zone stations show a difference in winter HDD between the NPO+ and NPO- phases that is significant at the 5% level. An additional two (Blythe and Long Beach) would be considered significant were the criterion relaxed to the 10% level. Only San Bernardino shows no wintertime effect of the NPO.

During summer, the relationships tend to be weaker. Out of the twelve climate zone stations, three are significant at the 5% level and another one (San Diego) would be included at the 10% level. It should be kept in mind, though, that the preceding winter value for the NPO is used when evaluating the summer conditions. This is therefore a kind of minimalist prediction scheme based on persistence.

b. Geographical pattern of correlation with the NPO

In addition to the shifting histograms at various stations, it is interesting to examine how the pattern of correlation varies across all stations in the state. This is shown in Figure 5 for winter (left panel) and summer (right panel) seasonal average temperature anomalies. Note that this is the correlation of actual temperature anomaly, not of HDD/CDD as shown previously. It has been suggested (e.g., Sailor and Munoz 1997) that the so-called ”primitive variables” such as temperature correlate to energy use better than derived variables such as HDD/CDD, so it is useful to examine both. The basis of the correlations is the winter (DJF) NPO index; therefore it is a simultaneous correlation for the DJF temperature anomalies, while the correlations for the JJA temperatures are based on the preceding winter.

Both summer and winter correlations are generally positive, which means that positive phases of the NPO are associated with warmer summers and winters. In winter, the correlations are strongest along the coast, and in the northern part of the state. This is in accord with the mechanism of the NPO, as described in section

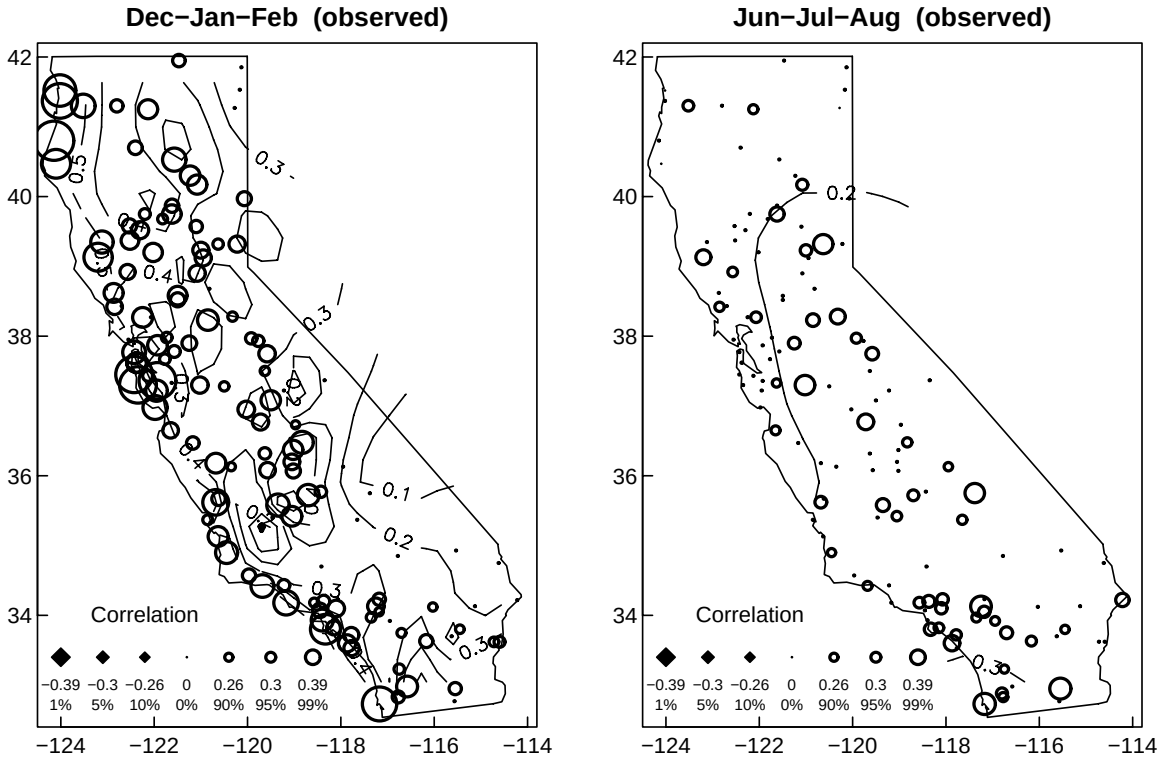

Figure 5: Observed correlation between the DJF NPO index and daily average temperature anomalies for the contemporaneous DJF (left panel) and the following JJA (right panel).

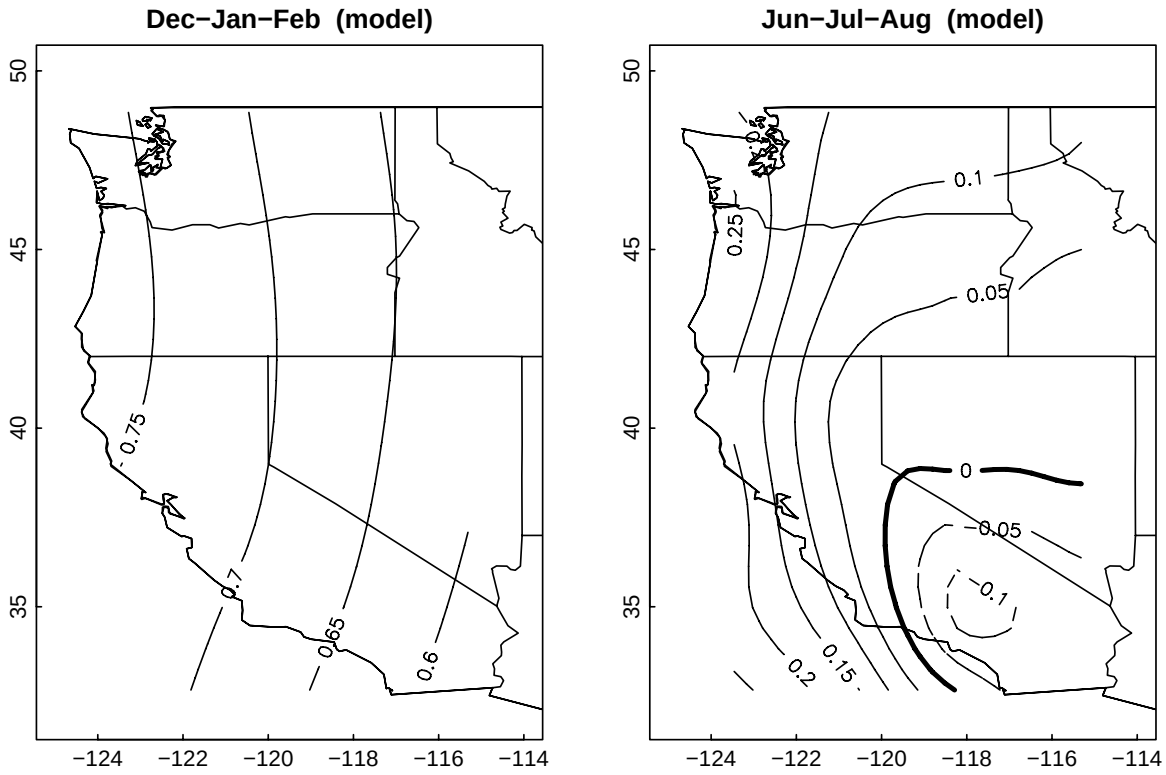

Figure 6: The model's correlation between the DJF NPO index and monthly average temperature anomalies for the contemporaneous DJF (left panel) and the following JJA (right panel).

2.1.

The correlation between the PCM's NPO index and monthly average temperature anomalies is shown in Figure 6. The most obvious difference between the model and observed results is that the reported correlations with the simultaneous DJF temperatures (left panel) is much stronger in the model than in the observations. However, keep in mind that the observed correlations are with daily temperatures, while the model correlations are with seasonally averaged temperatures (daily temperatures were not kept for the long model control run used here, so a direct comparison is not possible). This averaging will naturally result in greater correlation, as the random effects of unpredictable storms are smoothed over. Overall, it is certainly true that the model reproduces a strong NPO-driven

signal in temperatures over California, and that this is a feature of the observations as well, particularly in winter. In summer (right panel of Figure 6), the model correlations are weaker than observed, even with the averaging. This suggests that the model is missing an important part of the summer NPO-driven response over California.

c. Composite Temperature Maps

The correlations shown above are useful in that they are independent of possible changes in amplitude of the response. I.e., it could be imagined that a coastal city and an inland city might have approximately the same correlation with the NPO index, but the coastal city might have a smaller overall swing in temperature due to the NPO because of the nearby, moderating influence of the ocean. Also, correlations assume linearity (i.e., that the response to a low NPO condition is exactly opposite that to a high NPO condition), which may not be true. For both these reasons, it is useful to examine actual temperature composites based on the NPO index as well.

Figure 7 show the seasonal temperature anomalies composited for the upper (top row) and lower (bottom row) terciles of the NPO index. Figure 8 is similar, but the units are in degree days. Considering first the the high state of the NPO, the winter response (top left panel of Figure 7) shows a monotonic warm response over California. The amplitude of the response is greatest (approaching 1 C) over the northern mountainous regions, with the most moderate response (0.4 C) over the San Francisco bay area. In the following summer (top right panel of Figure 7), the amplitude of the response drops to 0.2 C or less. Additionally, there is a negative response in a narrow band of coastal cities, which seems to push into the interior near the San Francisco bay. This is potentially important from the point of view of the energy industry, as the San Jose “swing” region (so named because hot temperatures there can dramatically affect peak state energy use in summer) lies in this oppositely-signed region.

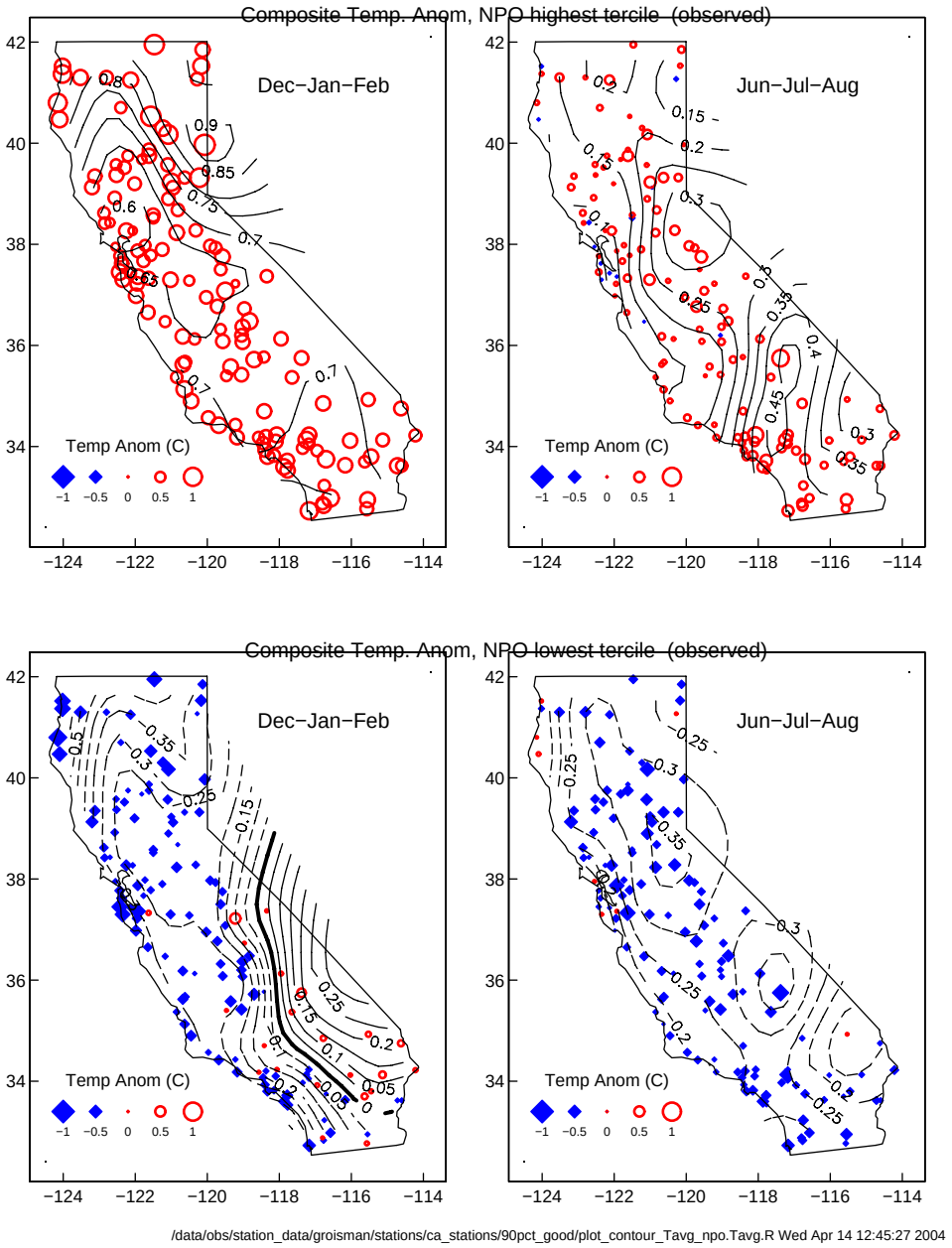

Figure 7: Observed seasonal mean temperature anomalies (^{o}C) composited on terciles of the winter (Dec-Jan-Feb) NPO index. Top row: for the highest tercile of the NPO index. Bottom row: for the lowest tercile. Left column: for the contemporaneous winter (Dec-Jan-Feb) season. Right column: for the subsequent summer (Jun-Jul-Aug) season. Contour interval is 0.05 C; negative contours are dashed. Dots indicate location of the stations used.

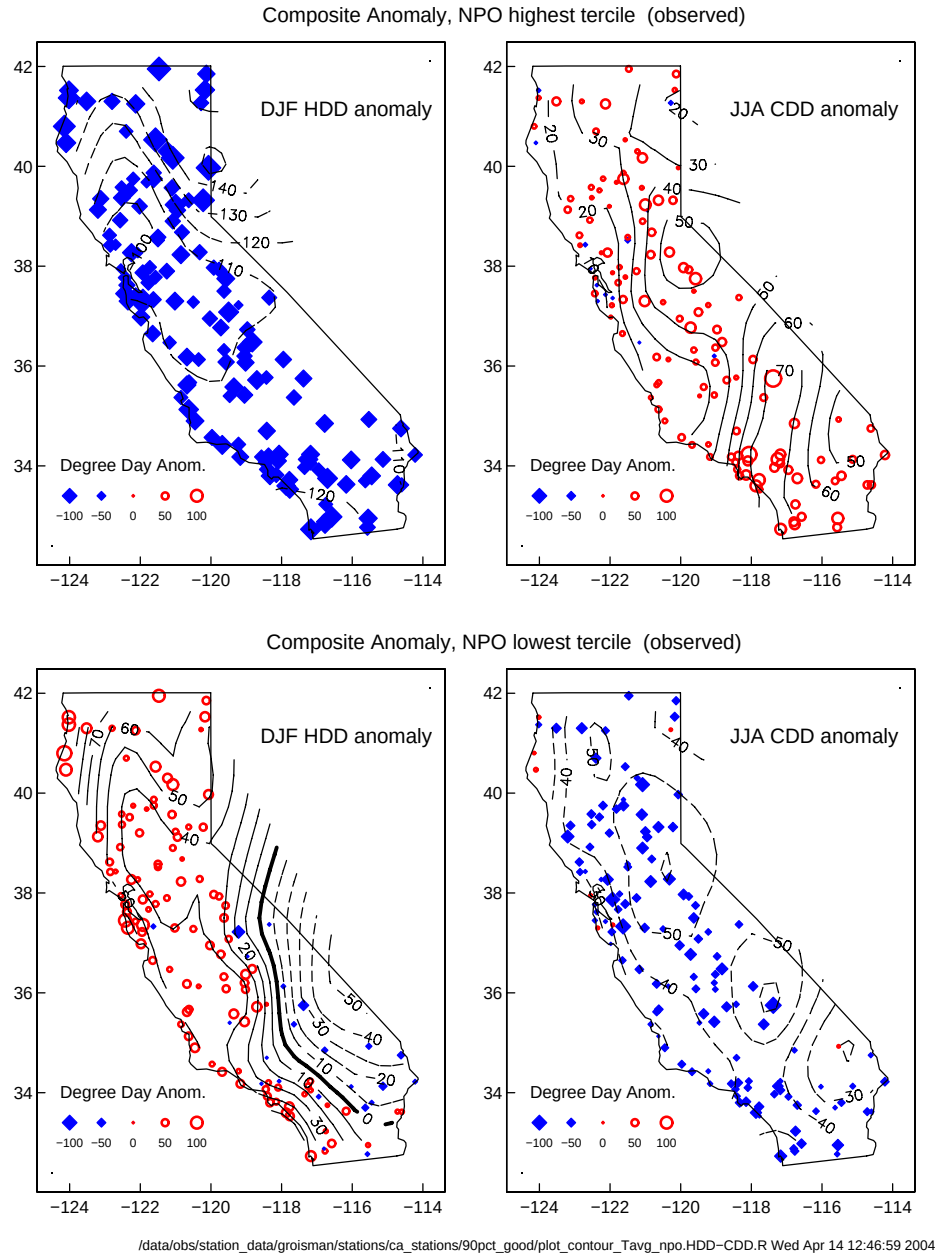

Figure 8: Observed seasonal mean heating and cooling degree day anomalies composited on terciles of the winter (Dec-Jan-Feb) NPO index. Top row: for the highest tercile of the NPO index. Bottom row: for the lowest tercile. Left column: for the contemporaneous winter (Dec-Jan-Feb) season. Right column: for the subsequent summer (Jun-Jul-Aug) season. Contour interval is 10 degree days; negative contours are dashed. Dots indicate location of the stations used.

The composite seasonal average temperature anomalies for low NPO conditions are shown in the bottom row of Figure 7. First off, it is clear that during winter, the response during low NPO conditions (lower left panel) is not simply the opposite of the response during high NPO conditions (top left panel). The response is distinctly weaker during low NPO conditions, with cold anomalies over the bulk of the north-central state being about -0.25 C, compared to +0.5 or greater when the NPO is high. Secondly, the response is not uniform across the state. The inland desert regions experience a positive response, while coastal regions and northern California experience a negative response. This is not clearly brought out in the correlation maps because of the intrinsically linear nature of that analysis. For the summer following low NPO conditions (lower right panel), the response is near uniform over the state, with conditions about 0.3 C cooler than the mean. There is no sign of a distinct local response over the San Francisco bay area during the summer following low NPO conditions, unlike the summer following high NPO conditions.

Figures 9 and 10 show the analogous figures generated using the model data instead of the observed dat. The model's response is somewhat weak during high NPO events in the winter (with modeled temperature anomalies in the range of 0.4 to 0.6^{o}C, observed anomalies 0.7^{o}C), and somewhat too strong during low NPO events (model: –0.4 to –0.6^{o}C; observed: 0.0 to –0.3^{o}C). In general, the model has a very symmetric response, such that the temperature anomaly field when the NPO is in the highest tercile is close to the negative of the field when the NPO is in the lowest tercile. The real world shows more non-linearities than the model manages to capture, with the high NPO response over California being distinctly stronger than the low NPO response.

d. Differences in daily temperature

The previous sections deal with seasonal differences in average temperature, and generally show that high NPO conditions are associated with warming over

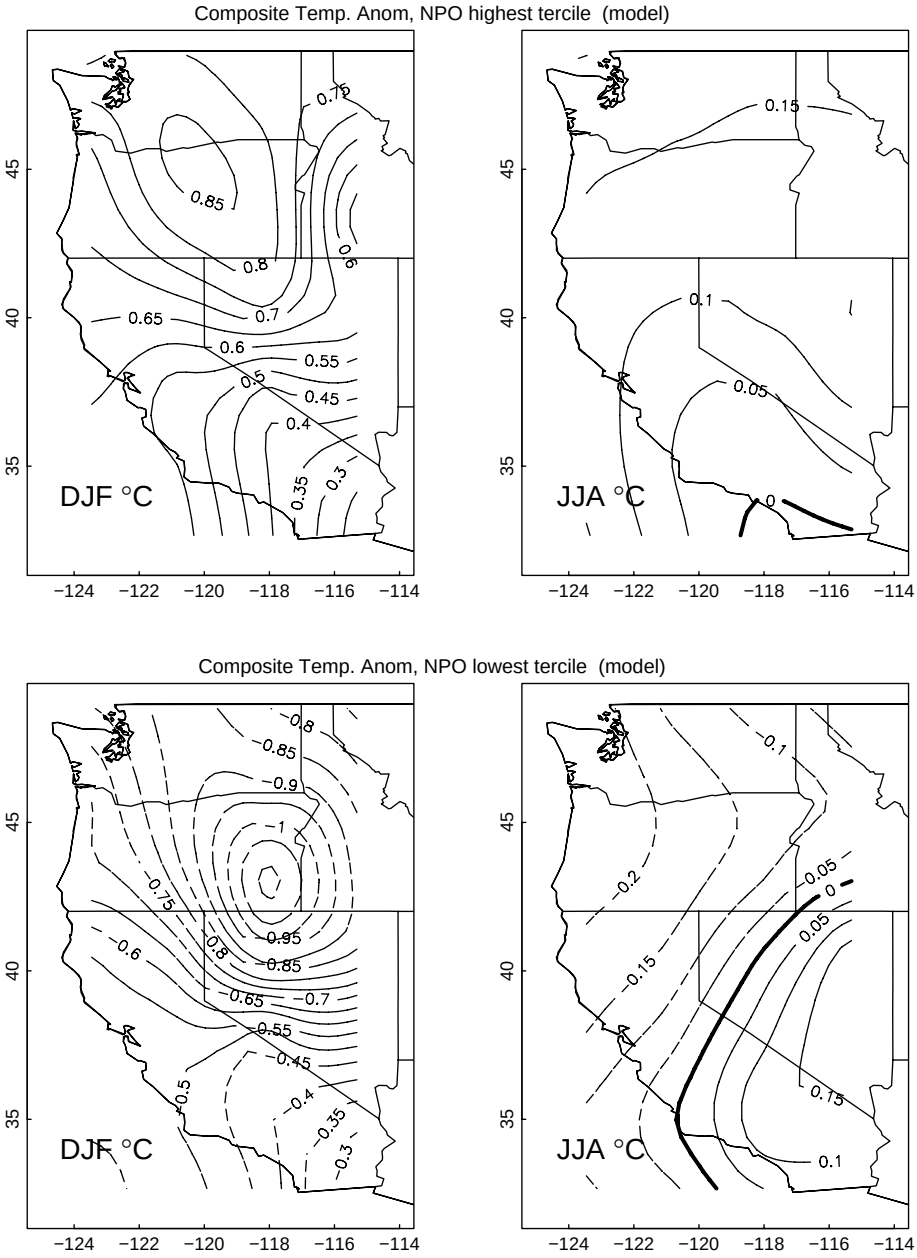

Figure 9: Model seasonal mean temperature anomalies (^{o}C) composited on terciles of the model's winter (Dec-Jan-Feb) NPO index. Top row: for the highest tercile of the NPO index. Bottom row: for the lowest tercile. Left column: for the contemporaneous winter (Dec-Jan-Feb) season. Right column: for the subsequent summer (Jun-Jul-Aug) season. Contour interval is 0.05 C; negative contours are dashed. Dots indicate location of the stations used.

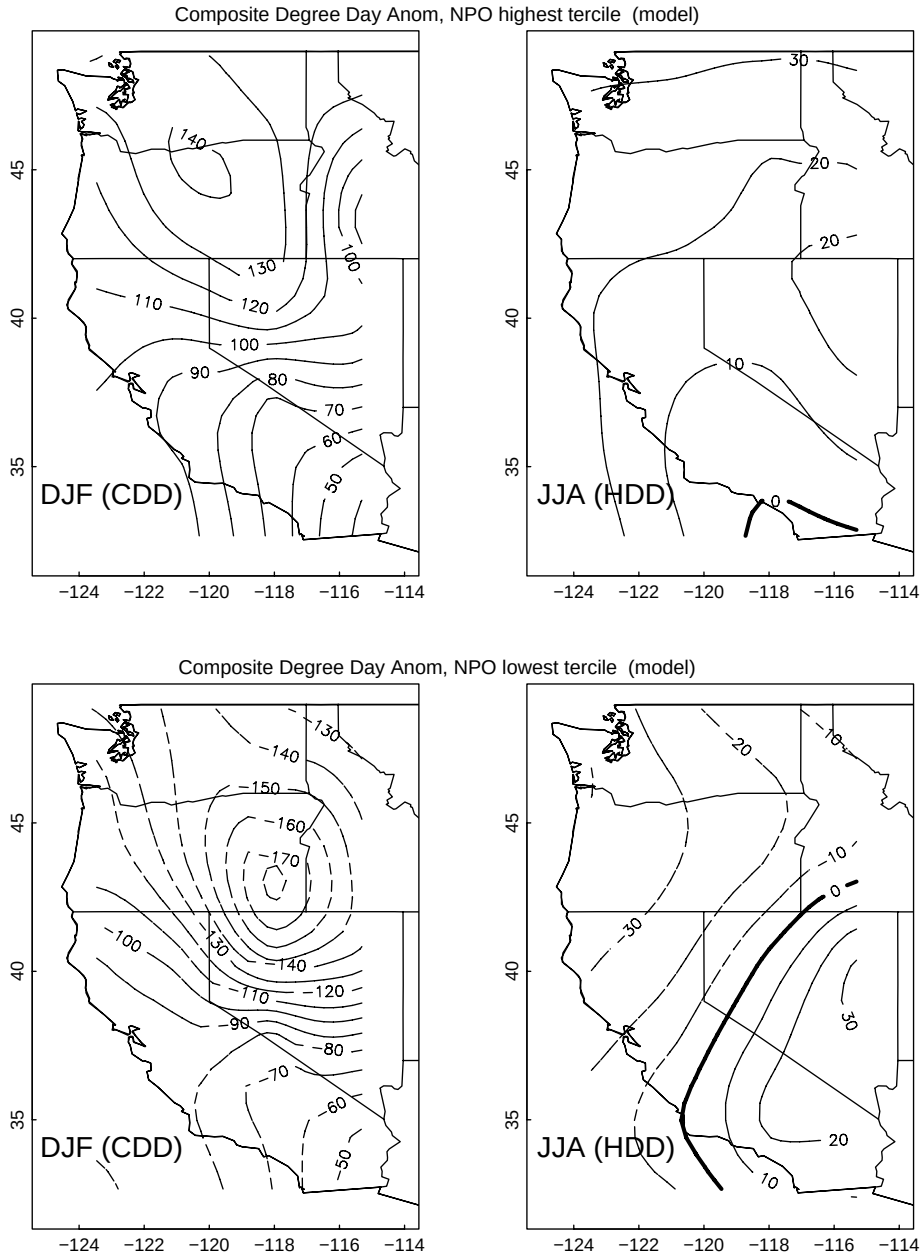

Figure 10: Model seasonal mean heating and cooling degree day anomalies composited on terciles of the model's winter (Dec-Jan-Feb) NPO index. Top row: for the highest tercile of the NPO index. Bottom row: for the lowest tercile. Left column: for the contemporaneous winter (Dec-Jan-Feb) season. Right column: for the subsequent summer (Jun-Jul-Aug) season. Contour interval is 10 degree days; negative contours are dashed. Dots indicate location of the stations used.

the state, while low NPO conditions are associated with cooling. However, for the purposes of energy producers, the manner in which the warming and cooling is accomplished is important. For example, were the winters warmer because of the lack of especially cold winter days, or because of a surfeit of particularly warm winter days? Or was the change accomplished simply by a uniform shift in the distribution of daily temperatures, with little change to the warm or cold tails of the distribution? Each possibility could potentially lead energy producers to a different strategy for dealing with the situation.

The way in which the change in seasonal average temperature is accomplished can be examined by comparing the distributions of daily average temperature obtained during the high and low NPO terciles. The mean of the distributions is first removed, since for this purpose we want to examine whether the shape of the distributions is different. This can again be evaluated by a K-S test, as was done before.

The results of this analysis are shown in Figure 11. Plotted are the significance values estimated by the K-S test for the difference in shape seen between the distributions of daily average temperature anomaly when the NPO is high and when it is low. Low values indicate that the difference in shape between the daily distributions is more than would be expected due to sampling fluctuations alone. We are using here an a priori significance test, which means that 1% of the stations would be expected to turn up as significant at the 0.01 level by chance alone. For winter conditions (DJF – left panel), 8 of the 134 stations (6%) show a significant difference at the 0.01 level; 24 (18%) are significant at the 0.05 level, and 41 (31%) are significant at the 10% level. Since three to six times as many stations are found to be significant as would be expected by chance, this analysis supports the idea that the NPO can lead to changes in the shape of daily temperature distributions, rather than simply shifts with no change in shape. Figure 11 shows that these changes are not uniform across the state. Rather, they are seen in a band stretching along the Sierra Nevada from northern California down to central California, then

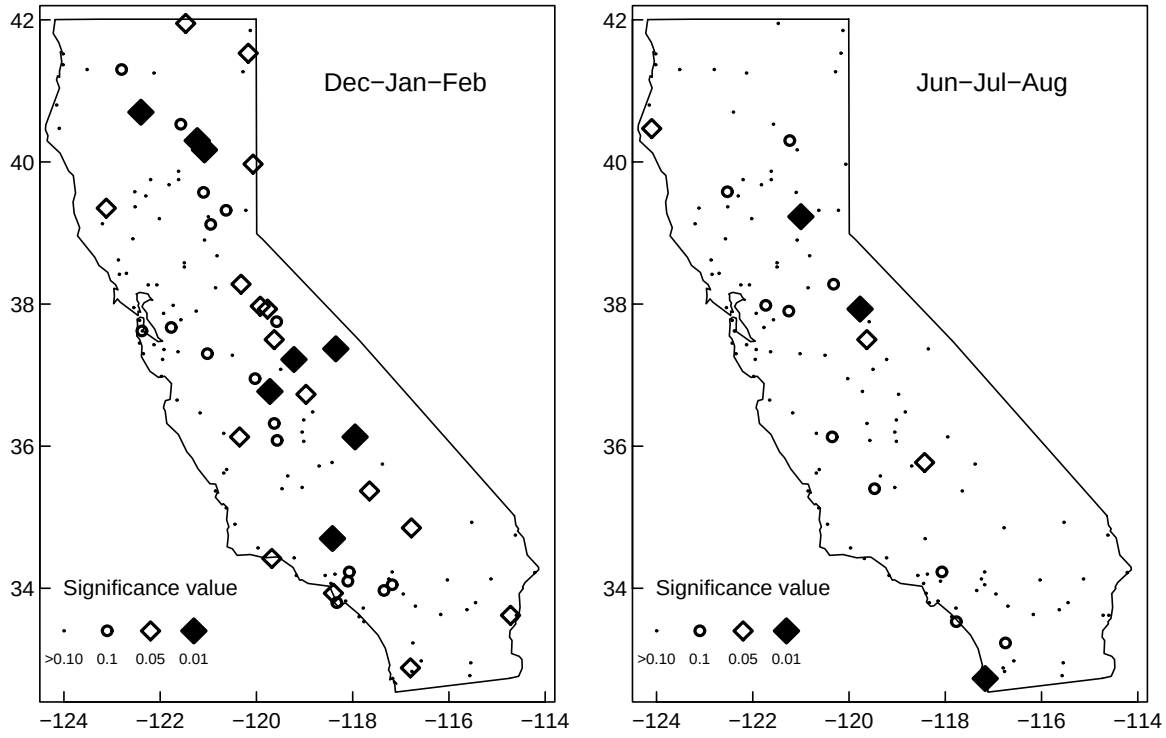

Figure 11: Significance values testing whether daily average temperature distributions have the same shape during high and low NPO conditions. Small significance values indicate differences between the distributions that were unlikely to have arisen from chance. See text for details.

swinging westward into the Los Angeles basin. The summer results (right panel) are distinctly weaker, with only 3 of 134 stations (2%) significant at the 0.01 level, 6 (4.5%) significant at the 0.05 level, and 16 (12%) significant at the 0.10 level. These are not particularly different from what would be expected due to chance, given the a priori statistics.

5. Influence of ENSO on California temperatures

In this section the effect of ENSO on California temperatures will be shown in a manner analogous to the NPO, for both the observations and the model.

a. Histograms of HDD and CDD by phase of ENSO

The main effects of ENSO that arise from the teleconnected response to tropi-

cal Pacific forcing are felt during the winter over North America. However, there may also be a more locally-forced response due to changes in SST during the summer, so the analysis will include the summer season as well. It should be noted that, in keeping with traditional usage of "El Nino" (warm tropical Pacific) and "La Nina" (cool tropical Pacific) events, this analysis will use a cutoff of 0.5 C for the Nino 3.4 index. In other words, El Ninos will be defined as the Nino 3.4 index being greater than 0.5 C, and La Ninas as the index being less than -0.5 C. This is in contrast to the analysis using the NPO index, where the histograms were constructed based merely on the sign of the NPO index, and the subsequent analysis was done on terciles of the NPO index.

Figure 12 shows the HDD and CDD distributions for El Nino and La Nina, at the representative California climate stations (Table 1).

The most striking thing compared to the NPO results (Figure 4 is the relatively weak effect ENSO has on California temperatures, compared to the effect of the NPO. Only a few stations have a statistically significant response, even in winter, while most of the stations did for the NPO.

This can easily be seen in the correlation of seasonal average temperature at each station with the Nino 3.4 index (Figure 13). The values are much weaker than the NPO values (Figure 5). In other words, ENSO generally accounts for less of the variability in California seasonal average temperatures than does the NPO. (It should be kept in mind that ENSO has much more influence on the precipitation.) The model results (Figure 14) are similar, although a somewhat stronger relationship between ENSO and wintertime temperatures is found.

Composite temperature anomalies that correspond to the phases of ENSO are shown in Figure 15, while the corresponding heating and cooling degree day anomalies are shown in Figure 16. Both contours and the actual composite temperatures at each station are shown; this gives complete information at the expense of some clarity. Over most of California, El Nino is associated with somewhat colder winters (upper left panel of Figure 15). The exceptions to this are the bay

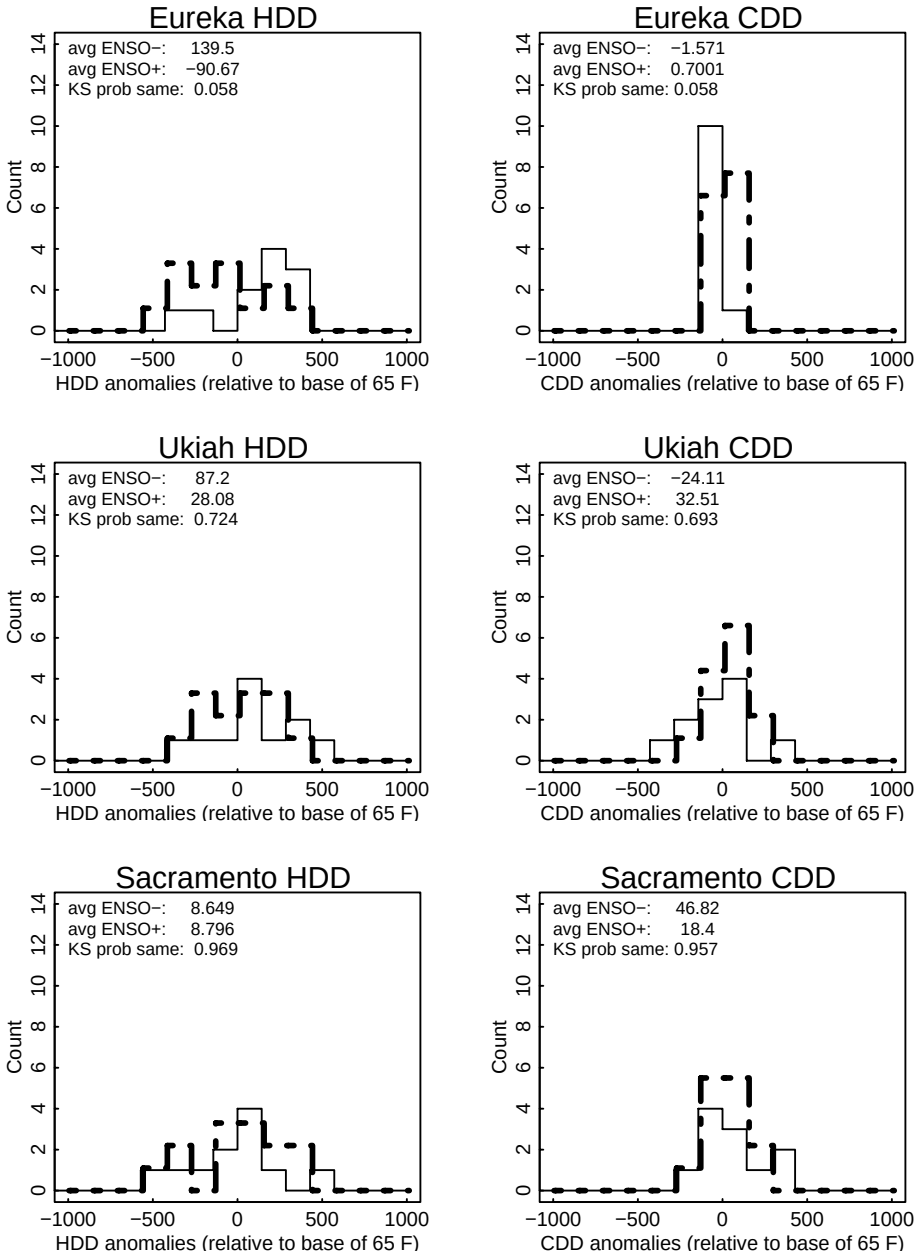

Figure 12a: HDD (left column) and CDD (right column) distributions for stations representative of California climate zones. The distribution for El Nino are shown by the heavy dashed line; for La Nina, by the thin solid line. Data has been detrended before analysis; departures from mean conditions are shown. HDD values are winter (Oct-March) average, CDD values are summer (May-Sep) averages.

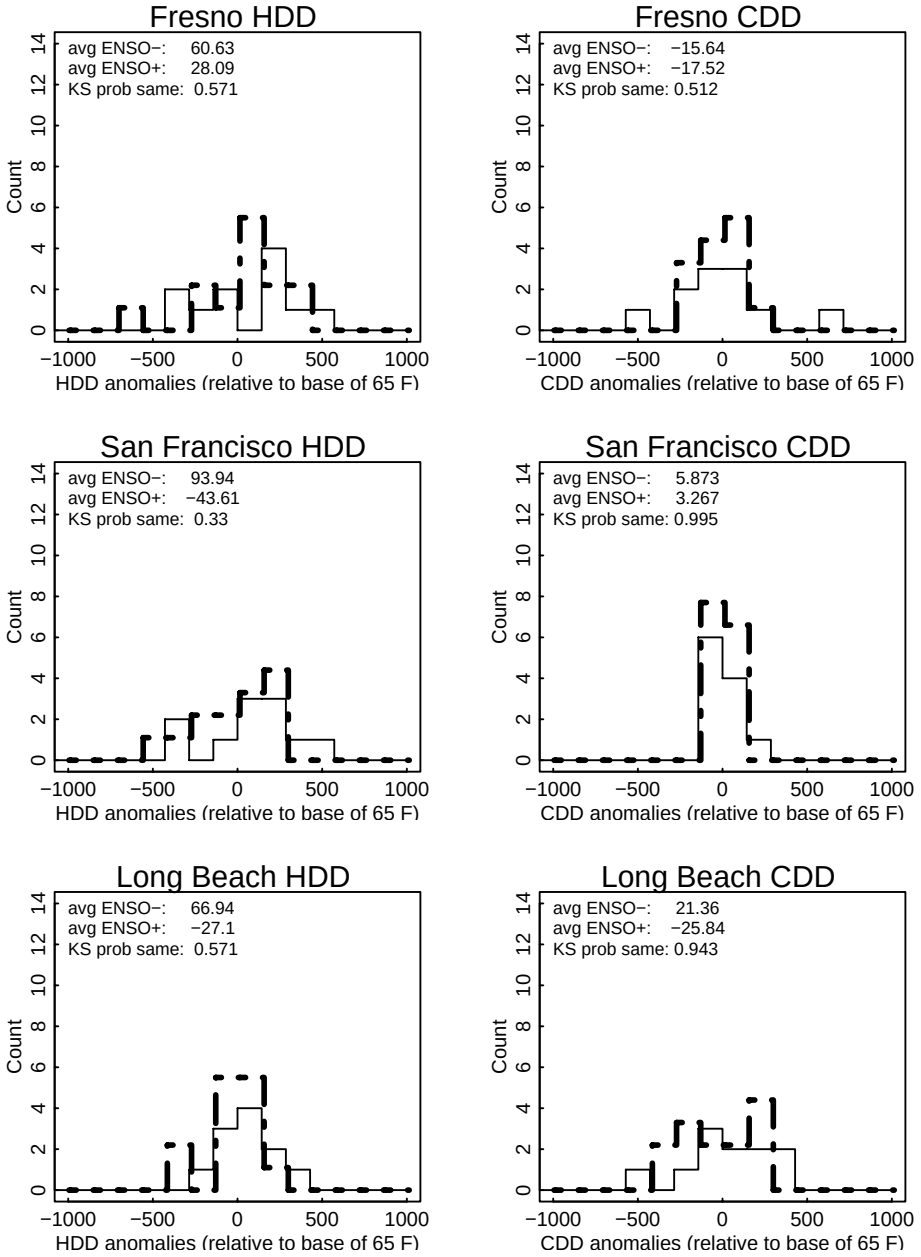

Figure 12b: continued.

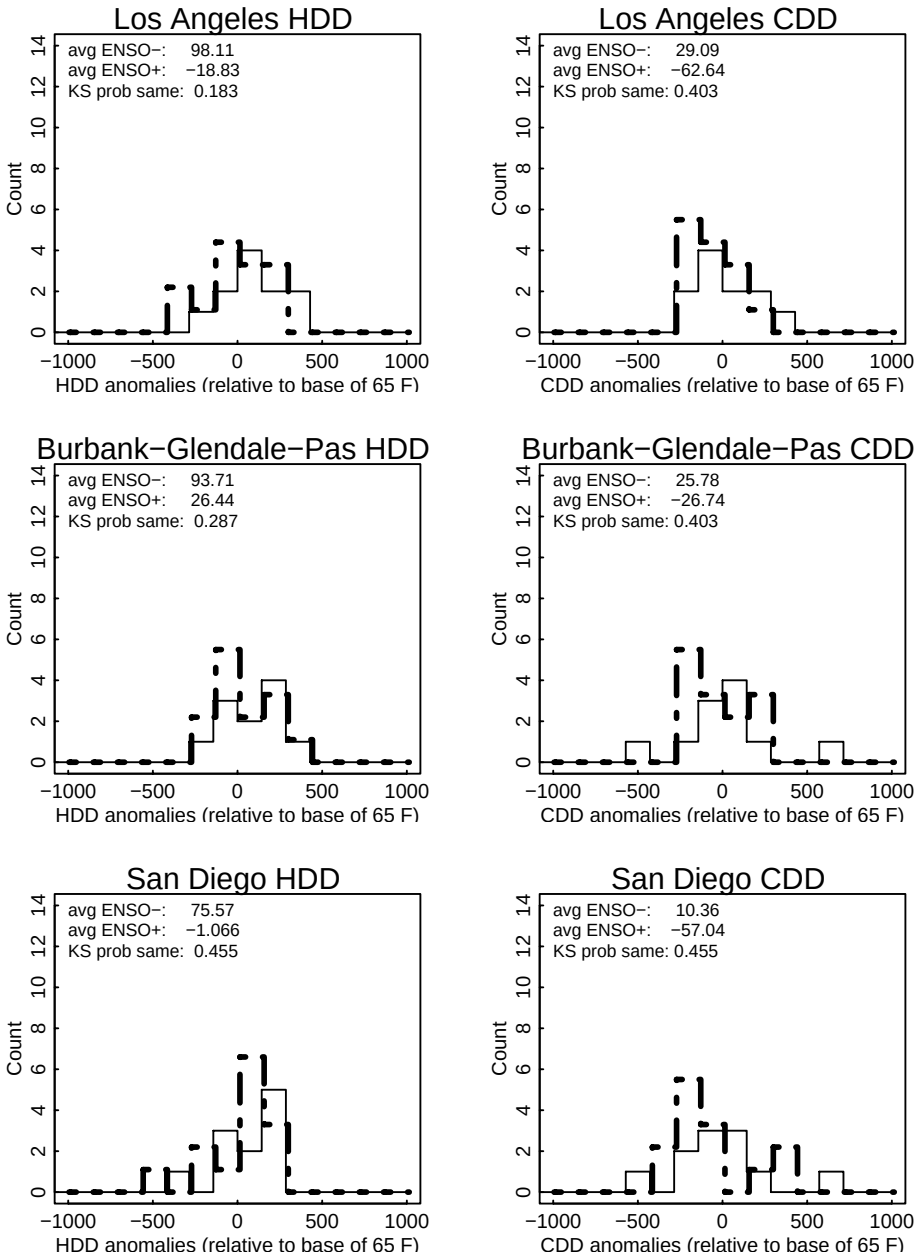

Figure 12c: continued.

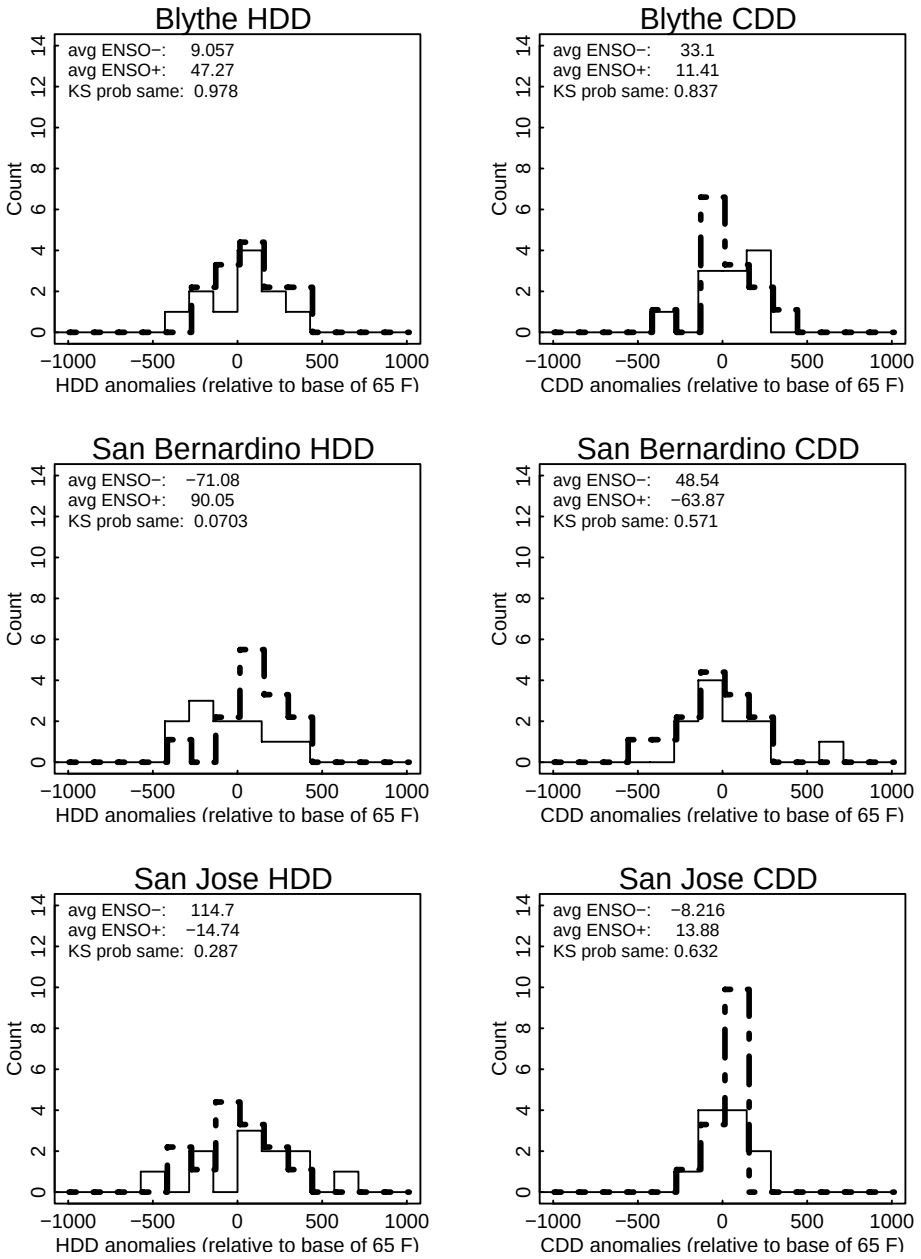

Figure 12d: continued.

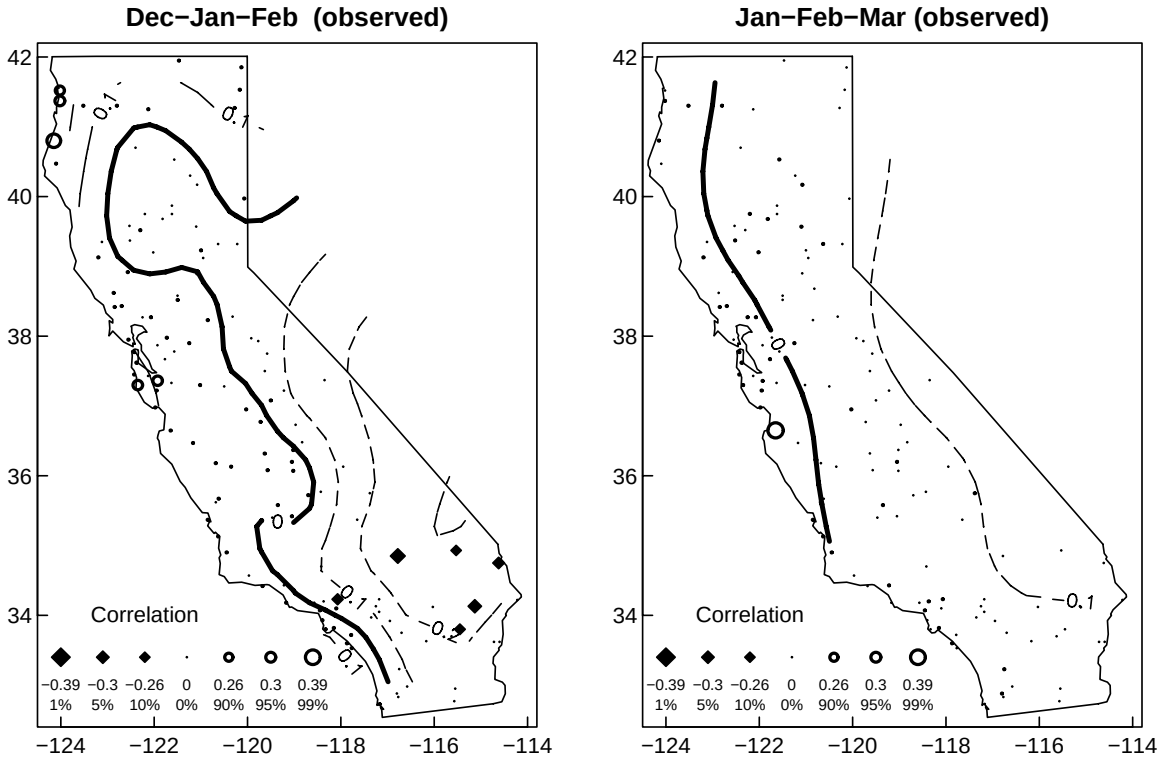

Figure 13: Observed correlation between the Dec-Jan-Feb Nino 3.4 index and daily average temperature anomalies for the contemporaneous DJF (left panel) and the following JJA (right panel).

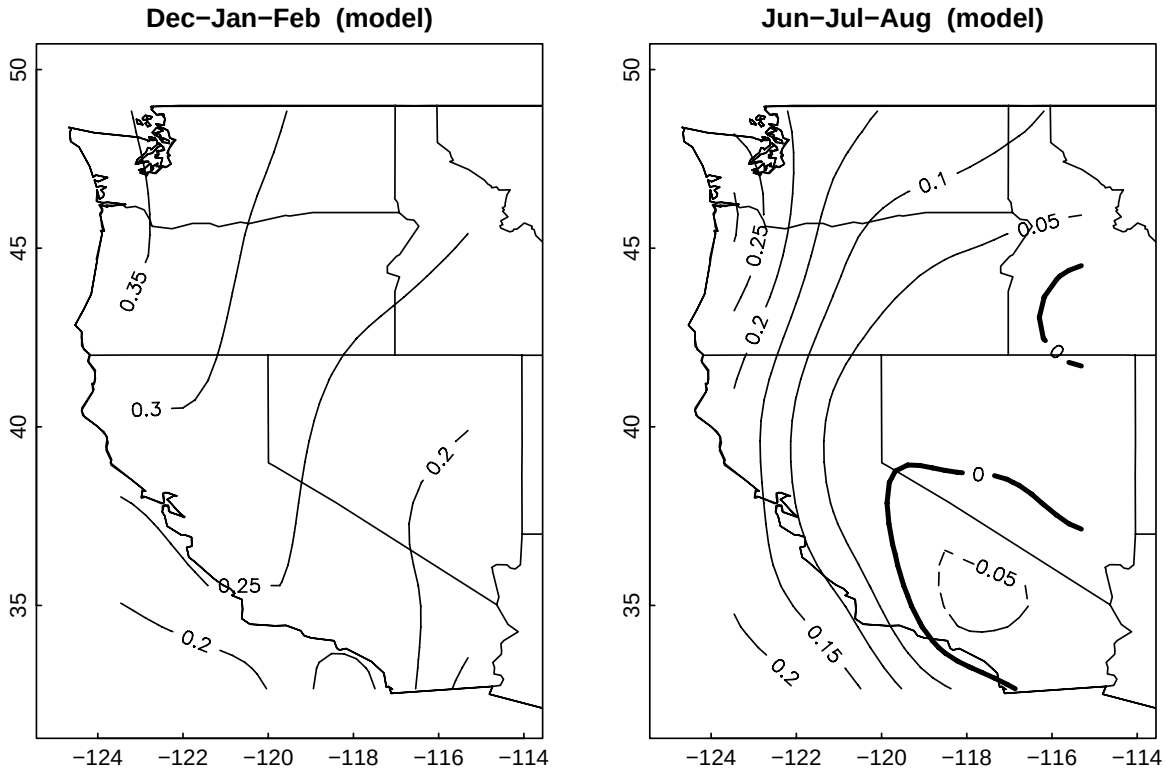

Figure 14: Model correlation between the Dec-Jan-Feb Nino 3.4 index and daily average temperature anomalies for the contemporaneous DJF (left panel) and the following JJA (right panel).

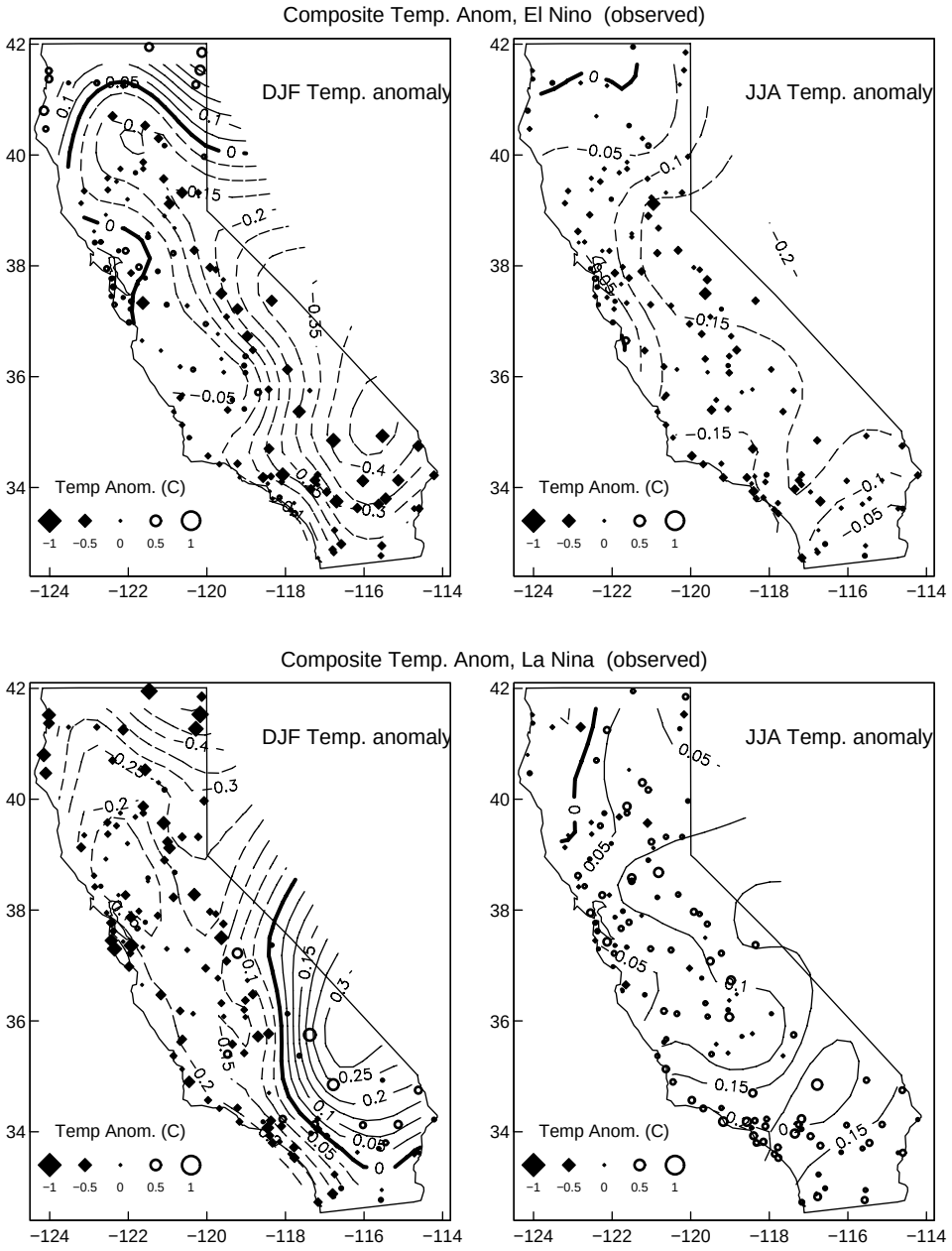

Figure 15: Observed temperature anomalies (degrees C) composited on the winter (Dec-Jan-Feb) Nino 3.4 (ENSO) index. Top row: for El Nino conditions. Bottom row: for La Nina conditions. Left column: for the contemporaneous winter (Dec-Jan-Feb) season. Right column: for the subsequent summer (Jun-Jul-Aug) season. Contour interval is 0.05 C; negative contours are dashed.

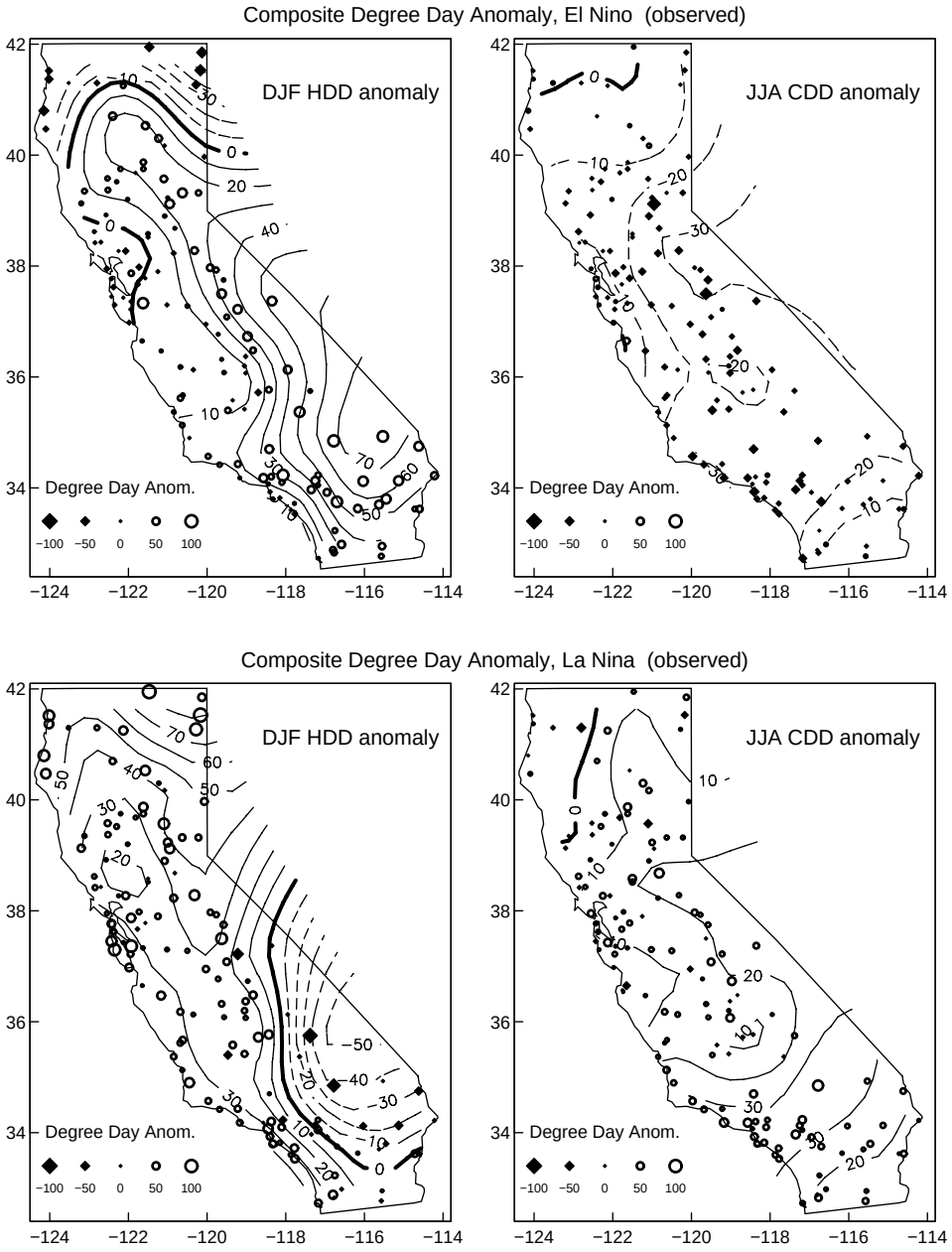

Figure 16: Observed heating and cooling degree day anomalies composited on the winter (Dec-Jan-Feb) Nino 3.4 (ENSO) index. Top row: for El Nino conditions. Bottom row: for La Nina conditions. Left column: for the contemporaneous winter (Dec-Jan-Feb) season. Right column: for the subsequent summer (Jun-Jul-Aug) season. Contour interval is 10 degree days; negative contours are dashed.

area, far northern California, and the few stations in southern California directly next to the ocean. The La Nina response is again generally cooler winters than average over much of the state, with the exception in this case being the interior southern part of the state. Responses during the summer following an El Nino or La Nina event tend to be more uniform (right hand column of Figure 15), with slightly cooler summers following El Nino and slightly warmer summers following La Nina, but this is a weak effect.

The model results for ENSO composite temperatures are shown in Figures 17 and 18 for completeness, but again it must be kept in mind that the response is too weak to be statistically significant. This likely accounts for the discrepancies seen between the model and observed values; for instance, the observations show a weak cool response in winter to an El Nino, while the model shows a weak warm response. Neither is significant.

6. Summary

The effect of the North Pacific Oscillation (NPO) and the El Nino-Southern Oscillation (ENSO) on seasonal average temperatures in California has been shown, using both observed station data covering 1960 to 2001 and the output of a 600-year control run of the Parallel Climate Model (PCM). Generally speaking, the NPO has a stronger effect on California's seasonally averaged temperatures than does ENSO, with predominately warmer winters when the NPO is positive and colder winters when the NPO is negative. The response in the following summer (Jun-Jul-Aug) is weaker than the simultaneous winter relation, but has the same sign (warmer with positive NPO, cooler with weaker NPO).

Although it varies by station, averaged over all of California the NPO makes a difference of about 150 HDD during the winter season. This is about a 5% effect.

The model has a reasonably accurate depiction of the NPO, with the noticeable downside that the model response is more linear than observed. Specifically, the model response to negative NPO conditions is almost opposite the response to

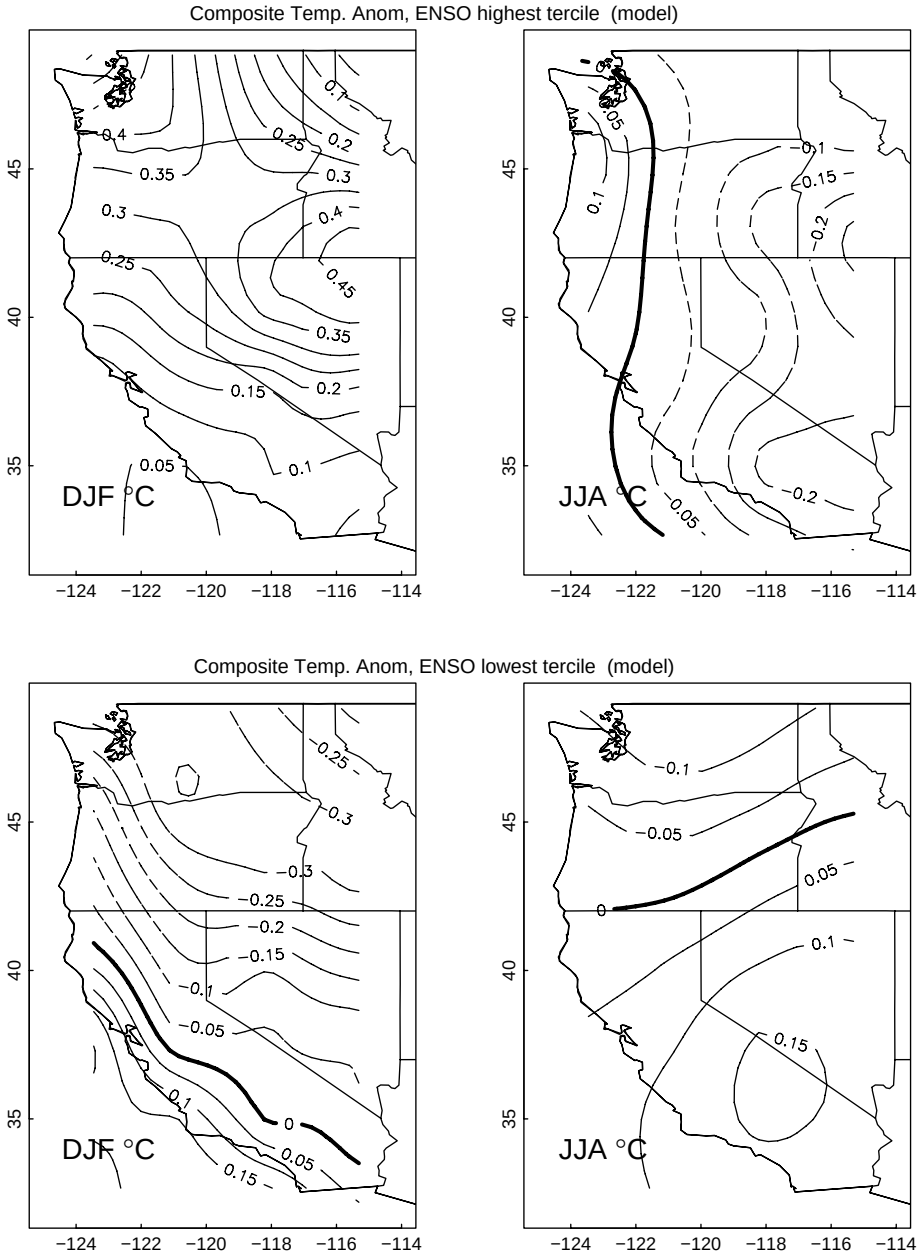

Figure 17: Model temperature anomalies (degrees C) composited on the winter (Dec-Jan-Feb) Nino 3.4 (ENSO) index. Top row: for El Nino conditions. Bottom row: for La Nina conditions. Left column: for the contemporaneous winter (Dec-Jan-Feb) season. Right column: for the subsequent summer (Jun-Jul-Aug) season. Contour interval is 0.05 C; negative contours are dashed.

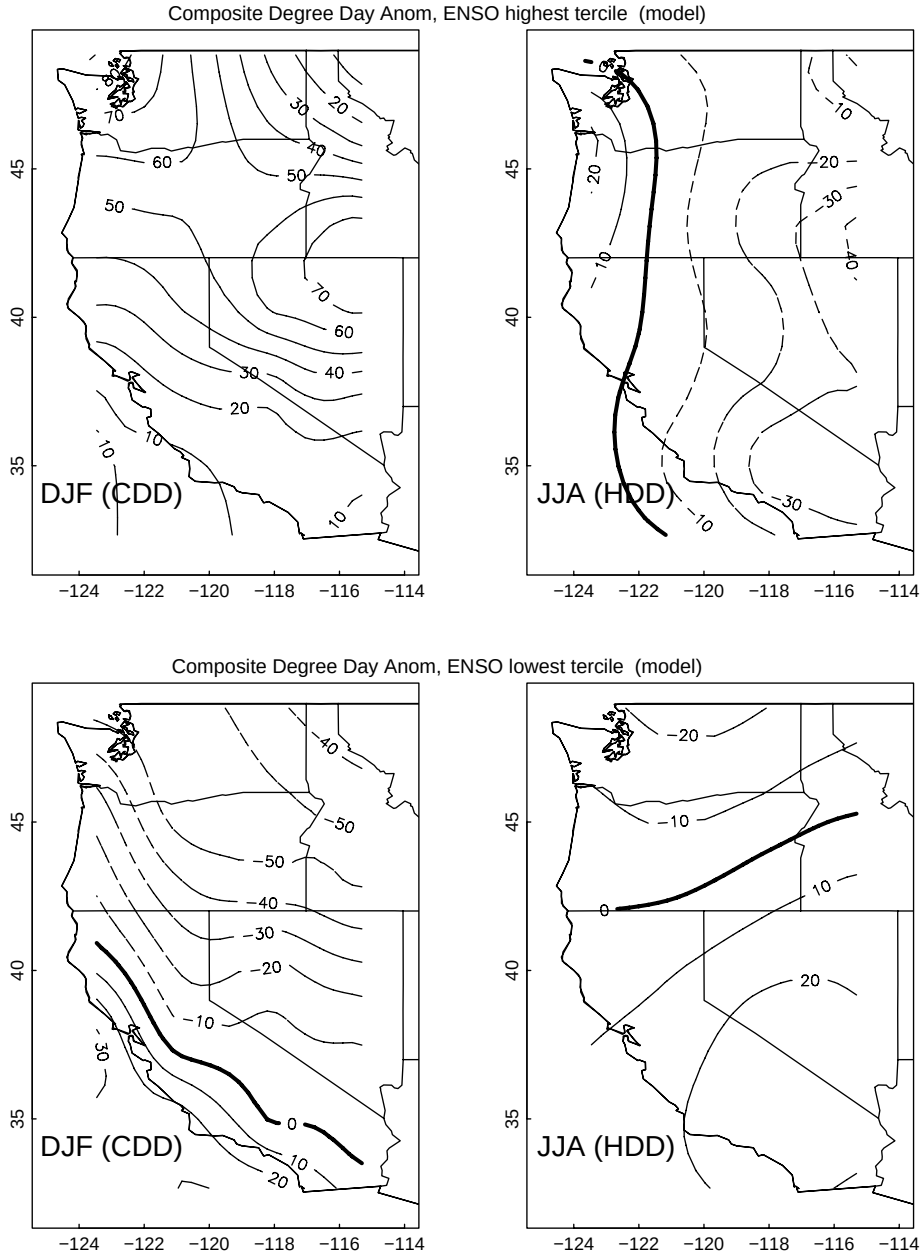

Figure 18: Model eating and cooling degree day anomalies composited on the winter (Dec-Jan-Feb) Nino 3.4 (ENSO) index. Top row: for El Nino conditions. Bottom row: for La Nina conditions. Left column: for the contemporaneous winter (Dec-Jan-Feb) season. Right column: for the subsequent summer (Jun-Jul-Aug) season. Contour interval is 10 degree days; negative contours are dashed.

positive NPO conditions, while in the observations, the response to negative NPO conditions is distinctly weaker than to positive NPO conditions. This suggests that the model's projections for winter response in conditions of negative NPO should be taken with a grain of salt. The model and the observations disagree as to the response in California temperature to an ENSO event, however, since neither response is statistically significant, it should be assumed that the source of this difference is sampling variability.

7. Acknowledgements

The analysis in this work would not have been possible without the sponsorship of the California Energy Commission under the California Applications Project (CAP), and of NOAA under the California Energy Security Project. The model runs were generated and obtained as part of the Accelerated Climate Prediction Initiative (ACPI) program, funded by the Department of Energy under grant DE-FG03-98ER62505. The runs were performed at the National Partnership for Advanced Computer Infrastructure (NPACI) at the San Diego Supercomputer Center, with the help of Peter Arzberger and Giridhar Chukkpalli, and at Oak Ridge National Laboratory, with the help of John Drake. We acknowledge the Center for Computational Sciences-Climate and Carbon Research (CCS-CCR) at Oak Ridge for computational resources used to generate those model results.

References

Barnett, T. P., R. Malone, W. Pennell, D. Stammer, A. Semtner, W Washington, 2004: The effects of climate change on water resources in the west: Introduction and overview. *Climatic Change*, v. **62** p. 1-11.

da Silva, A. M., C. C. Young, S. Levitus, 1995: Atlas of Surface Marine Data 1994, Volume 1: Algorithms and Procedures. NOAA Atlas NESDIS 6, U.S. Dept. Commerce, 299 pp.

Latif, M., T. P. Barnett, 1994: Causes of Decadal Climate Variability over the North Pacific and North America. *Science*, v. **266** p. 634-637.

Mantua, N. J., S. R. Hare, Y. Zhang, J. M. Wallace, R. C. Francis, 1997: A Pacific Interdecadal Climate Oscillation with Impacts on Salmon Production. *Bull. Amer. Met. Soc.*, v. **78** p. 1069-1079.

Mechoso, C. R., A. W. Robertson, N. Barth, M. K. Davey, P. Delecluse, P. R. Gent, S. Ineson, B. Kirtman, M. Latif, H. Le Treut, T. Nagal, J. D. Neelin, S. G. Philander, J. Polcher, P. S. Schopf, T. Stockdale, M. J. Suarez, L. Terray, O. Thual, J. J. Tribbia, 1995: The Seasonal Cycle over the Tropical Pacific in Coupled Ocean-Atmosphere General Circulation Models. *Mon. Wea. Rev.*, v. **123** p. 2825-2838.

Pierce, D. W., 2001: Distinguishing Coupled Ocean-Atmosphere Interactions from Background Noise in the North Pacific. *Prog. Oceanogr.*, v. **49** p. 331-352.

Sailor, D. J., J. R. Munoz, 1997: Sensitivity of electricity and natural gas consumption to climate in the USA - Methodology and results for eight states. *Energy*, v. **22** p. 987-998.

Trenberth, K. E., J. W. Hurrell, 1994: Decadal atmosphere-ocean variations in the Pacific. *Climate Dynamics*, v. **9** p. 303-319.

Walker, G. T., E. W. Bliss, 1932: World weather V. *Mem. R. Meteorol. Soc.*, v. **4** p. 53-84.

Walker, G. T., 1923: Correlation in seasonal variations in weather III: A preliminary study of world weather. *Mem. Indian Meteor. Dept.*, v. **24** p. 75-121.

Washington, W. M., J. W. Weatherly, G. A. Meehl, A. J. Semtner, T. W. Bettge, A. P. Craig, W. G. Strand, J. Arblaster, V. B. Wayland, R. James, Y. Zhang, 2000: Parallel Climate Model (PCM) control and transient simulations. *Climate Dynamics*, v. **16** p. 755-74.

Released: February 2004

Level of review: Work in progress; please do not cite without author's permission.

In partial fulfillment of: California Energy Comission Contract No. 500-02-004
UC Campus Award No. MR-03-02
Task #5

Order copies of this report (free of charge) from:

CCCC/CAP Reports
Dept 0224, Scripps Instutution of Oceanography
9500 Gilman Drive, La Jolla, CA 92093, USA